SYNTHESIS OF BOROSILICATE GELS WITH PHENYL MODIFICATIONS

AND ITS EFFECTS ON PROTON CONDUCTIVITY

By

ANIRUDH TUMULURI

A thesis submitted to the

School of Graduate Studies

Rutgers, The State University of New Jersey

In partial fulfillment of the requirements

For the degree of

Master of Science

Graduate Program in Materials Science and Engineering

Written under the direction of

Lisa C. Klein

And approved by

_____

_____

_____

New Brunswick, New Jersey

October 2019

ABSTRACT OF THE THESIS

SYNTHESIS OF BOROSILICATE GELS WITH PHENYL MODIFICATIONS

AND ITS EFFECTS ON PROTON CONDUCTIVITY

By

ANIRUDH TUMULURI

Thesis Director:

Lisa C. Klein

Silicon alkoxides with boron alkoxides or boric acid were used to prepare borosilicate xerogels. Nitric acid was used to promote the hydrolysis of the silicon alkoxides, tetraethylorthosilicate (TEOS) and phenyltriethoxysilane (PhTES). Triethyl borate (TEB) and boric acid were the source of boron in the gels. The compositions were: 85 wt. % TEOS - 15 wt. % TEB, 80 wt. % TEOS - 15 wt. % TEB - 5 wt. % PhTES, 75 wt. % TEOS - 15 wt. % TEB, 10 wt. % PhTES, 85 wt. % TEOS - 15 wt. % Boric Acid, 80 wt. % TEOS - 15 wt. % Boric Acid - 5 wt. % PhTES and 75 wt. % TEOS - 15 wt. % Boric Acid, 10 wt. % PhTES.

Thermogravimetric Analysis (TGA) and Differential Scanning Calorimetry (DSC) were performed to investigate the loss of weight and heat flows in the gels as a

function of temperature. The weight loss and the energy absorbed during the endothermic peak decreased with the increasing PhTES content. Gels made from TEB show lower weight losses and enthalpy changes compared to similar gels made from boric acid.

X-Ray Diffraction was performed for phase identification and to determine the amount of crystallinity in the gels. The diffraction patterns contained peaks that were attributed to boric acid precipitates, which occurred in all the gels. Increase in PhTES decreased the amount of crystallinity in the gels. Gels made from TEB show lower amounts of crystallinity compared to similar gels made from boric acid.

Moisture adsorption-desorption was performed to investigate the water retention capabilities of the gels. The increases in PhTES content decreased the water retained in the gels. Adsorption values of the gels made from TEB and boric acid are comparable, but the mass loss due to desorption are higher for the gels synthesized from boric acid.

Electrochemical Impedance Spectroscopy (EIS) was performed to measure the proton conductivity of the gels. The increase in PhTES content reduces the proton conductivity slightly. Proton conductivity is dependent on the number of protons and the number of sites available for hopping of protons. The phenyl in PhTES decreased the number of protons and sites. Gels prepared from TEB show higher proton conductivity compared to same gels made from boric acid.

ACKNOWLEDGMENTS

TABLE OF CONTENTS

LIST OF TABLES

LIST OF FIGURES

I. INTRODUCTION

A proton conductor is an electrolyte, typically a solid electrolyte, in which H^+ ions (protons) are the charge carriers. There are aqueous acid solutions, such as aqueous sulfuric acid, that exhibit high proton conductivity in ambient pressure and temperature. In particular, the focus here is solid electrolytes, including polymer electrolytes and ceramic electrolytes. The pores in these electrolyte materials are small such that the protons on the surface and in bulk contribute to direct current conductivity and ionic transport [1].

Proton conductivity is pivotal in processes as diverse as photosynthesis in green plants and the production of electricity in a hydrogen fuel cell. Recently, fuel cell systems using proton-conducting electrolytes have garnered much attention owing to their high energy conversion efficiency at low temperatures without the emission of harmful pollutants. A series of perfluorosulfonate ionomers (e.g., NAFION) have received much consideration as possible electrolytes, and research efforts in these electrolyte materials have continued over the past two decades. Although perfluorosulfonate ionomers exhibit high proton conductivity, their industrial applications are limited by high costs and insufficient electrochemical stability [2]. This has prompted a great interest in development of proton conductive glass electrolytes which are generally composed of silicate glass networks and mixed acid species. It might seem that glass is a typical insulator and not appropriate as an electrolyte, but phosphosilicate glasses have shown conductivity values comparable to that of perfluorosulfonate ionomers. Considering the chemical and thermal stabilities

along with low fabrication costs, inorganic glass membranes have potential as the electrolyte of fuel cells [3].

Borosilicate glass contains substantial amounts of silica (SiO_2) and boron trioxide ($B_2O_3 > 8\%$) as glass network formers, and are typically composed of 70-80 wt.% SiO_2, 7-13 wt.% B_2O_3. Glass containing 7-13 wt.% B_2O_3 is known as low borate borosilicate glass, and is mainly used to produce chemical apparatus, lamps and tube envelopes. Glasses containing 15-25 wt.% B_2O_3 are known as high borate borosilicate glass. High B_2O_3 (>15%) significantly alters the behavior of the glass, making it thermal shock resistant, which allows the glass to resist rapid changes in temperature without cracking. Secondly, the increase of B_2O_3 content, within the silica phase increases the chemical resistance as the boron in the silica phase makes it less soluble, preventing any unwanted materials from leaching into the glass and for this reason, they are widely adopted materials for storage and immobilization of nuclear waste. In principle, borosilicate glasses seem to fulfil the shortcomings of the perfluorosulfonate as well as offering the desired properties for its use as a fast proton conducting electrolyte.

The sol-gel process is performed in two different ways. The first route involves destabilizing a colloidal suspension by changing the pH of the system so that gelation occurs. The colloid can be dispersed in either polar or non-polar media, or acetates or nitrates can supply the other metal cations in multicomponent systems.

In the second technique, metal alkoxides are first hydrolyzed in alcoholic solutions by atmospheric moisture or by direct addition of water that usually contains an acidic or a basic catalyst. A condensation/polymerization reaction immediately follows the hydrolysis reaction, and the hydrolyzed species are converted into

polymers that are soluble in the alcoholic solutions. The polymers in the solution continue to grow and eventually crosslink and encompass the solution. At this stage the gel point has been reached and is generally irreversible for the process using metal alkoxide [4].

In this study, the sol gel method using metal alkoxides was utilized in making borosilicate gels because of the offered advantages - high purity of cations and anions, good solubility (homogeneity), and ability to hydrolyze and polymerize easily. The gels were prepared using two different boron precursors along with phenyl group modifications to the silicon precursor. The effects of the synthesis parameters on the proton conductivities have been studied.

II. LITERATURE SURVEY

2.1 SOL-GEL PROCESSING OF GLASSES WITH METAL ALKOXIDES

The increasing demands continuously placed on the glass technology to produce materials with stringent property requirements necessitates the synthesis of chemically pure materials. Sol-gel process using metal alkoxides has generated considerable interest in the recent years to meet this expectation.

Sol-gel process can produce glasses without melting as the constituents are supplied by metal alkoxides. The constituents of the glass are supplied by the metal alkoxides, and in some cases metal salts of acetates and nitrates. Acetates and nitrates are particularly used to supply metal ions of group IA and IIA.

The usage of the term 'Metal Alkoxides' is often mixed up with 'Organometallic' compounds. Metal alkoxides are members of the family of metalorganic compounds, which have an organic ligand attached to the metal or the metalloid atom whereas organometallic compounds are defined by the direct metal-carbon bonds unlike metal-oxygen-carbon linkages in metal alkoxides [5].

Initially, the metal alkoxide, in this case for silicon, $(Si(OR)_4)$ is hydrolyzed according to the following reaction:

$$Si(OR)_4 + H_2O \rightarrow Si(OR)_3\text{-}OH + ROH$$

The R represents a proton or other ligand (if R is an alkyl group, then OR is an alkoxy group, and ROH is an alcohol). Depending on the amount of water and catalyst present, the hydrolysis may stop (partial hydrolysis) or go to completion.

$$Si(OR)_4 \; + \; 4H_2O \quad \rightarrow \quad Si(OH)_4 \; + \; 4ROH$$
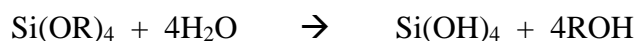
Partially hydrolyzed species are immediately accompanied by a condensation reaction as follows:

$$(OR)_3\text{-}Si\text{-}OH \; + \; OH\text{-}Si(OR)_3 \quad \rightarrow \quad (OR)_3Si\text{-}O\text{-}Si(OR)_3 \; + \; H_2O$$

or

$$(OR)_3\text{-}Si\text{-}OR \; + \; OH\text{-}Si(OR)_3 \quad \rightarrow \quad (OR)_3Si\text{-}O\text{-}Si(OR)_3 \; + \; ROH$$
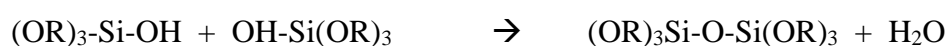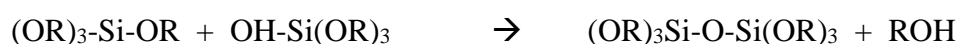
Although the polymerization process represented above appears to be simple, it is likely that polymerization is quite complex and involves several polymeric species. A variety of monomers have been found to exist in the solution and eventually polymerize into dimers, trimers, and other oligomers. As the polymers continue to grow, they crosslink and eventually form a gel.

The gel is then subjected to drying to remove alcohol and physically adsorbed water. At this stage, the gel has interconnected porosity, and its surface is covered with hydroxyl groups. The dried gel is referred to as xerogel which can be converted to a glass by heat treatment below the liquidus temperature.

The attractions to making glass through sol-gel processing are numerous, especially for the compositions that are difficult to form by conventional melting. Primary advantage of this method is the processing of similar composition glasses at lower temperatures as opposed to fusion. The lower processing temperature widens the range of glass compositions by allowing volatile materials to be incorporated

along with overcoming the problems of crystallization is some systems [6]. In addition, the lower fabrication temperature could potentially allow for the glasses to be formed that have a stable and metastable liquid-liquid immiscibility zones such as $CaO-SiO_2$ [7] and $La_2O_3-SiO_2$ [8].

Another key attraction is that the metal alkoxides, are typically liquids at room temperature. This leads to improved purity in the glass (i.e., fewer metallic impurities) as the alkoxides can be distilled before using. Also, the homogeneity of the multicomponent systems can be improved as the metal alkoxides are mixed on an atomic level.

2.2 SOL-GEL DERIVED BOROSILICATE GLASSES

Borosilicate gels have been made through sol-gel processing using both methods: destabilizing suspensions of colloidal silica and by hydrolyzing and polymerizing metal alkoxides. Borosilicate gels made by destabilizing colloidal suspension will be covered first, followed by a review of borosilicate gels made from metal alkoxides.

2.2.1 SOL-GEL DERIVED BOROSILICATE GLASSES MADE BY DESTABILIZING COLLOIDAL SUSPENSIONS

Jabra [9] made glasses in the $SiO_2-B_2O_3$ systems by destabilizing an aqueous silica sol that was mixed with an aqueous solution of ammonium tetraborate. Once the suspension gelled, it was dehydrated at 175˚C for fifteen hours followed by hot pressing. Glasses were made with boria contents ranging from 5 to 50% and

properties such as density, refractive index, thermal expansion were similar to glasses of similar compositions formed by outside vapor phase oxidation. Rabinovich et al. [10] made glasses containing 96% silica (SiO_2-B_2O_3) by gelling a colloidal silica/water gel. Boron was added later as an aqueous solution of boric acid. The suspensions were dispersed, dried, and redispersed so that monolithic rods could be formed without breakage. The gels were sintered at 1450˚C, and the properties were comparable to that of fused glasses of similar composition.

2.2.2 SOL-GEL DERIVED BOROSILICATE GLASSES MADE FROM METAL ALKOXIDES

The sol-gel process using metal alkoxides to form borosilicate gels involves hydrolysis followed by condensation of the alkoxide complexes that contain both boron and silicon or by first hydrolyzing a silicon alkoxide and subsequently adding boron alkoxide. The former process has been attributed to the work of Dislich [11], while the latter has been credited to a method initially developed by Levene and Thomas [12] and later by Yoldas [13].

When forming a complex metal alkoxide, the individual alkoxides forming the complex are generally stirred and heated to ensure copolymerization. Bradley [14] cited many examples of complex metal alkoxides that can be made by reacting metal alkoxides.

Russak [15] made a soda-lead-borosilicate glass with an alkoxide complex made by reacting tetraethylorthosilicate (TEOS = $Si(OC_2H_5)_4$) with trimethyl borate (TMB = $B(OCH_3)_3$). This complex was partially hydrolyzed with HCl catalyst, and a

metal salt solution containing nitrates of lead and sodium was then added to the complex. The gel was then dried, pulverized and then melted. The homogeneity of the gel was found to be superior for all the times and temperatures involved with melting.

Decottignies [16] also prepared borosilicate using a metal alkoxide complex. TEOS and TMB were reacted in ethanol at 60˚C for four hours to form the complex. A pre-calculated amount of water was added to the complex to ensure hydrolysis, and the solution was gelled at room temperature.

When silicate glasses are made from alkoxides, silicon alkoxide is hydrolyzed first because of its slow hydrolysis rate. This holds true even for borosilicate glasses as the silicon alkoxide hydrolyzes much more slowly than the boron alkoxide. The partially hydrolyzed species of silicon alkoxide contain silanol groups (SiOH) which can react with other alkoxides, and for this reason, it is important to let the silicon alkoxide hydrolyze first to increase the number of silanol sites formed. The reaction is usually aided with the addition of an acidic or basic catalyst.

Addition of the faster hydrolyzing alkoxide to the silicon alkoxide with inadequate silanol groups can cause the faster hydrolyzing alkoxide to self-polymerize resulting in a species that cannot be reacted with other components. Nevertheless, the hydrolysis of silicon alkoxide should not be allowed to proceed for too long as the silanol groups formed condense into siloxane polymers and are no longer available to react with other alkoxides. The two competing effects require the addition of the faster hydrolyzing alkoxide during an optimum time range where maximum number of silanol groups are available.

2.3 PARAMETERS OF THE SOLUTIONS AND THEIR EFFECTS ON THE DRIED GEL

The ratio of the water, alcohol, and the alkoxide in the solution plays a critical role in determining the structure of the dried gel. First the effect of pH on the hydrolysis reaction mechanism is discussed, followed by the role of water to alkoxide ratio, solvent and the temperature of the solution. Lastly, the effect of reesterification in solutions and its resultant effect on the dried gel structure is described.

2.3.1 EFFECT OF pH ON THE HYDROLYSIS REACTION

The mechanism for the hydrolysis of silicon alkoxide depends on the pH of the solution of water, alcohol, and alkoxide. In acidic solutions an electrophilic reaction mechanism is responsible for hydrolysis, while in basic solution hydrolysis results from nucleophilic substitution reaction.

In an acidic solution, a water molecule is protonated and approaches the oxygen atoms in the basic alkoxy groups attached to the silicon alkoxide. In this mechanism, an activated complex is proposed where the hydrogen atoms on the protonated water molecule form partial bonds with the oxygen atoms in the alkoxy groups. From this transition state, two of the partial bonds formed strengthen to form a silanol and alcohol molecule while a proton is released.

With silicon alkoxides, the most highly esterified species, the alkoxy groups are most likely to be hydrolyzed in an acidic solution. This is because of the high electron density around the silicon atom because of basic nature of the alkoxy groups. As one of the alkoxy groups is removed by hydrolysis, the electron density around the

silicon atom decreases, making this species less attracted to a positive hydronium ion. This decrease in electron density because of alkoxy group removal should make tetra-alkoxy group species prone to attack by a hydronium ion followed by end alkoxy groups on polymer chains and then by middle alkoxy groups on polymer chains.

Sakka and Kamiya [17] presented evidence that the polymers formed in acidic solutions tend to be linear and weakly branched by measuring the reduced viscosities of Si(OR)$_4$ solutions formed with varying amounts of water and concentrations of HCl or NaOH. The extent of linear polymer formation in acid solution is subject to the amount of water used in hydrolysis and the temperature of the solution. Brinker et al. [18] further corroborated this study by analyzing both acidic and basic hydrolysis of TEOS using small and X-ray scattering. Using the intermediate angle scattering region, Brinker was able to obtain information on the structure of polymer species.

In alkaline solutions, the hydrolysis of a silicon alkoxide occurs by a bimolecular nucleophilic substitution reaction. Under basic conditions a hydroxyl group attacks the backside of a tetra-alkoxy monomer. The attacking nucleophile and the departing alkoxy group are located on the opposite side of the silicon atom. When the reaction is complete, the departing alkoxy group leaves on the opposite side of the newly formed Si-OH bond, and the molecule is inverted as a result of the reaction.

In a basic medium, tetra-alkoxy monomer is the most difficult species to hydrolyze because of the high electron density surrounding the silicon atom when the alkoxy groups are present. The high electron density tends to repel the hydroxyl groups and limits hydrolysis. However, once an alkoxy group is removed, the electron density surrounding the silicon atom decreases, making the monomer more

susceptible to hydrolysis. Polymers formed in alkaline solutions are more highly branched than those formed in acidic solutions.

2.3.2 WATER TO ALKOXIDE RATIO

The amount of water used to hydrolyze an alkoxide varies anywhere between a molar water to alkoxide ratio of 1:1 to 30:1. This ratio has significant effect on the type of polymer that is formed in the solution and consequently affects the structure of the dried gel.

In general, as the water content increases the polymers formed are more likely to branch. In alkaline solutions, a high water to alkoxide ratio has the most pronounced effect on branching. The combined effect of a basic solution and large water content leads to the formation of branched, cluster like polymers. The result of increasing the water to alkoxide ratio is shown to increase the oxide content of silica gels [19].

In contrast, low water contents (water to alkoxide ratio of 4 or less) produce polymers that are linear and weakly branched. This primarily results from the encounter rate between the alkoxide and water decreasing as the water to alkoxide ratio is lowered. With the decreased encounter rate, the polymerization reaction starts long before the alkoxide is completely hydrolyzed. This effect is most notable for acidic solutions of low water content.

The type of polymer formed results from the combination of water content and pH. For instance, relatively branched polymers can be formed in acidic solutions if high water content is used. Therefore, a general guideline for the type of polymer

found in solution is that acidic solutions of low water content tend to yield linear, weakly branched polymers while basic solutions with high water to alkoxide ratio yield polymers that are highly branched.

2.3.3 ROLE OF SOLVENT

Since water and alkoxides are immiscible, it is necessary to use a common solvent to bring them into solution. The most commonly utilized solvents are alcohols. However, any family of organic liquid capable of hydrogen bonding with water can be employed, such as amines, amides, or ketones.

Most of the work done on sol-gel processing has employed methanol or ethanol as solvent. The solvent chosen should have the same carbon chain as the ligands of the alkoxide, to prevent the possibility of ligand exchange. For instance, if ethyl alcohol is used as a solvent with methyl alkoxide, it is possible for the ethyl group to replace the methyl group. This ligand exchange is of critical concern as it alters the starting raw materials, thereby affecting the hydrolysis rate.

The solvent has an important role in the drying of the porous gels. The stresses induced within the pores of the gel has been analyzed by Zarzycki et al. [20] and shown that the capillary pressure is proportional to the surface tension of the liquid and inversely proportional to the pore radius. Based on this relation, it is preferable to utilize a low surface tension solvent to enhance the feasibility of making gels.

The solvent viscosity is another important factor as it alters the solution viscosity. The viscosity of the solution controls the film thickness by the sol-gel dip

technique. In the case of bulk gels, viscosity is expected to affect the hydrolysis and polymerization kinetics. A high viscosity will decrease the mobility of the catalyst and reactants through the solution, thus slowing the reaction and increasing the gelation time [21].

2.3.4 AGING

Changes in the structure of a gel can occur even after gelation. The changes in the structure with time when solvent is not evaporating are referred to as aging.

One phenomenon that can take place is that the average polymer size increases with time. This results from small polymers having a higher solubility than larger polymers. The smaller polymers dissolve and redeposit on larger polymers.

Also, the bulk density of the dried gel is affected by aging. When polymers dissolve and redeposit at inter-polymer necks, the integrity of the gel network increases. On drying, the surface tension force causes the gel network to contract. If the solution and redeposition of polymers has taken place in the gel, the gel is less susceptible to contraction. Because of this, gels formed with high water content and high pH are more resistant to shrinkage on drying and have lower bulk densities than gels formed from solutions of low pH and low water content. This effect has been observed experimentally [22-24].

2.3.5 RE-ESTERIFICATION

On drying, the gel loses both alcohol and water. If the amount of alcohol present is greater than the amount of water, the reverse of hydrolysis reaction (re-esterification) can occur on drying.

As more water is lost on drying, the formation of fully esterified alkoxide molecule is favored. Re-esterification appears to be most prevalent for acidic solutions. This may explain the observation that although acid catalysed solutions are initially more hydrolyzed than basic solutions, re-esterification eventually causes hydrolysis to be less complete in acidic solutions than basic solutions. Also, re-esterification could explain the loss of boron in multicomponent gels. If boron is re-esterified to the highly volatile boron alkoxide, it can evaporate on drying and decrease the boron content of the gel.

2.4 FACTORS CONTRIBUTING TO HIGH FREE ENERGY OF THE ALKOXIDE GELS

In contrast to melt prepared glass, gels have relatively high free energies. The three major characteristics of alkoxide gels contributing to this high free energy are examined in this section.

Firstly, gels have high surface area. When an alcogel is desiccated, the meniscus formed, and the capillary forces pull the polymer structure of the gel together. Once, the gel is completely dried, a fine interconnected network of porosity remains. The porosity contained in gel is the source of high surface area. Surface area makes the largest contribution to the free energy of the gels.

Secondly, alkoxide gels have high free energy because of their low crosslink density. Alkoxide gels are not nearly as cross linked as melt prepared glasses. On heating, the alkoxide gel polymerizes, thereby removing some of the non-bridging oxygen atoms. However, depending on the Si-O-Si bond angle formed during the reaction, the heat of formation can be either exothermic or endothermic. Gibbs, using molecular orbital calculations, calculated the heat of formation for an edge sharing silicate, where the Si-O-Si bond angle is 87°, is +210 kJ/mol. The contribution to the free energy of a gel resulting from non-bridging oxygen atoms converting to bridging oxygen atoms is strongly dependent on the bond angle.

Lastly, alkoxide gels have a free volume larger than melt prepared glasses. The excess free volume results from the open structure frozen in at the gel point. On heating the gel in the glass transition range, the gel structure can exothermically relax towards a structure representing a melt prepared glass and reduce the excess free volume.

2.5 CONDUCTIVITY IN GLASSES

Conventional glasses are insulators at room temperature, but with an increase in temperature, there is an increase in conductivity for glasses. In contrast, metals which are conductive at room temperature have lower conductivity at increased temperature. While glasses can be both ionically and electronically conductive, in most cases ionic conduction is due solely to the movement of a single ionic species, either anion or cation. The electronic conductivity depends on mobility of the electrons while ionic conductivity depends on the mobility of charged ions. It is generally accepted that composition influences both conductivity and the mobility,

but there is no agreement on which changes the most from an insulator to a good conductor.

It is generally accepted that in many glasses, alkali ions move under the influence of an electric field. Therefore, glasses such as alkali silicate, alkali borate, and alkali borosilicate show ionic conduction. The conductivity of a glass containing only one type of charge carrier, for instance an alkali ion, can, in general, be described by the equation:

$$\sigma = \sigma_0 \exp(-E/RT)$$

where σ_0 is a pre-exponential factor, E the activation energy, R the gas constant and T the absolute temperature. The logarithmic version of this expression is usually referred to as the Rasch-Hinrichsen equation. As the temperature approaches the range where structural rearrangements become possible, the conductivity increases more rapidly with increasing temperature, usually leading to a second region where the Rasch-Hinrichsen equation applies with a higher activation energy [25].

The electrical conductivity of borosilicate glass is discussed below, followed by the comprehensive study of proton conduction in various systems along with recent advances in proton conducting glass electrolytes.

2.6 ELECTRICAL CONDUCTIVITY IN BOROSILICATE GLASS

The dependence of the activation energy of the electrical conduction on the composition of the glass is discussed by Stevels [26]. The activation energy is determined by the average height of potential barriers. In this way, one may explain the higher activation energy for K^+ ions in potassium-silicate glasses compared to the

activation energy for Na^+ ions in sodium silicate glasses up to a certain amount of alkali oxide. At higher alkali-oxide concentration the glass structure becomes less dense, the larger K^+ ions may now move more easily than the smaller Na^+ ions because the latter are bonded more strongly to the network. In general, a rapid increase of the conductivity is observed on addition of alkali oxide to vitreous silica up to about 20-30 mol % alkali oxide, although at higher concentrations the increase is less pronounced. This increase in conductivity can he directly related to the mobile alkali ions.

It is also known that thermal treatments in the annealing-transformation range have a significant influence on the electrical conduction of many glasses. Charles [25] showed the influence of phase separation or stress in the glass on the electrical conduction of glasses. The effect of the water content on the electrical conduction of sodium silicate glass was studied by Martinsen and McGee [27]. It was established that small numbers of hydroxyl ions increased the electrical conduction of the silicate glasses remarkably. Scholze and Mulfinger [28], based on diffusion experiments, proposed that H^+ ions jump from OH^- ions to a neighboring non-bridging oxygen ion and that the electrical charges are neutralized by simultaneous diffusion of OH^- ions. Such a reaction may also take place in the presence of an electric field giving rise to an increase in the conduction.

Han, Kreidle and Day [29] studied the electrical conduction in alkali-borate melts and showed that the electrical conduction in alkali-borate melts increased rapidly in the 15 to 50 mol % alkali-oxide range measured at the same temperature. Otto [30] measured the electrical conduction in sodium- and lithium-borosilicate glasses. The temperature dependence of the electrical conductivity was found to

follow the Rasch-Hinrichsen equation up to the softening range. Empirical formulae were derived to express the conductivity of glass with high alkali content as a function of the composition. The conductivity was increased by raising the alkali-oxide content, or, if the mole fraction of alkali oxide was kept constant, by increasing the concentration of SiO_2. Differences in conductivity were primarily caused by a change in the energy of activation. According to Otto [30], three concentration regions could he distinguished for the description of the activation energies. A rather steep but linear decrease was observed from 0 to 25 mol % alkali oxide at a constant mol % SiO_2. An abrupt change was observed at 25 mol % alkali oxide, and the activation energy still decreased linearly with increasing alkali-oxide content.

Ehrt and Keding [31] measured the electrical conductivity and viscosity of four simple sodium borosilicate glasses. Batches of sodium carbonate (Na_2CO_3), boric acid (H_3BO_3) and silicon dioxide (SiO_2) were mixed at melted at temperatures varying between 1300-1580°C, and the glasses were obtained by pouring the melt into a mold. The compositions of the samples varied over a wide range: 3–33 mol% Na_2O, 0-62.5 mol% B_2O_3 and 25-85 mol% SiO_2. It was observed that the electrical conductivity was strongly dependent on the content of Na^+ ions and their mobility through the glassy network. Sodium borosilicate glasses ($T \leq T_g$) had much lower electrical conductivity than sodium silicate glasses due to the special borate units. The Na^+ ions are more strongly bonded to BO_4^- tetrahedra with bridging oxygen than to SiO_3O^- tetrahedra with non-bridging oxygen. Above T_g, in the softening region, the electrical conductivity of sodium borosilicate glasses increases strongly and approaches the values of sodium silicate samples.

Muray [32] conducted experiments on the surface conductivity of borosilicate glass by projecting an electron beam onto a clean borosilicate glass surface in vacuum. As the electrons arrive at the surface, they are rapidly bound to lattice imperfections presumably creating O^- ions. However, there was no surface conduction by free electrons, and surface conductivity of clean glass was low and comparable with volume conductivity. It was concluded that the high apparent plasma induced surface conductivity was in the plasma, and not in the glass.

Lima, Monteiro, Graca, and da Silva [33] studied the structural, electrical and thermal properties of borosilicate glass - alumina composites and showed that the dc conductivity of all samples increased with sample temperature and Al_2O_3 content. The composite samples exhibited an increase in ac conductivity with the increase in the amount of Al^{3+} ions present in the glass structure as formers and modifiers.

The electrical conduction behavior of borosilicate glasses confirms the generally accepted view that alkali ions are the primary charge carriers below T_g. Above T_g, it cannot be excluded that small numbers of hydroxyl ions and protons take part in the conduction process so that an interpretation in terms of structural units is impossible.

2.7 PROTON CONDUCTION

Proton transport and transfer phenomena have been studied extensively from rather different points of view by material scientists, chemists, physicists, and biologists. It is beyond the scope of this review to address all of the systems for which proton conductivity has been reported. The proton is the only ion which has no

electron shell of its own. Therefore, it strongly interacts with the electron density of its environment, and then takes on some H 1s orbital character.

In metals, this environment is the delocalized electron density of the conduction band, where the proton is considered to be a part of a hydrogen with some protonic or hydridic character depending on whether the energy of the H1s state is higher or lower than the Fermi energy of the pure metal.

In non-metallic compounds, where there is a single oxygen, well separated from other electronegative species, this results in the formation of an O-H bond. The proton may be involved in two bonds: a short, strong bond with the proton donor and a longer, weak bond with a proton acceptor. It is interesting to note that electronically conducting oxides as a host for protons seem to represent a transition between these limiting cases of proton bonding. Whereas the proton forms a hydroxyl ion with one oxygen in electronically insulating oxides, the presence of a high concentration of conduction electrons leads to a breaking of the OH bond.

Two principal mechanisms describe proton diffusion in such a way that the proton remains shielded by some electron density along the entire diffusion path. In the first case, the proton migration is assisted by the translational dynamics of bigger species. The proton diffuses together with a "vehicle" (e.g., as H_3O^+) where the counter diffusion of unprotonated vehicles (e.g., H_2O) allows the net transport of protons [34].

In the other case, the "vehicles" show pronounced local dynamics but reside on their sites, the protons being transferred within hydrogen bonds from one vehicle to the other. Additional reorganization of the proton environment, which comprises, e.g., reorientation of individual species or even more extended ensembles, then results

in the formation of an uninterrupted trajectory for proton migration. The proton conductivity in water containing systems is explained in detail, followed by a brief review of the conductivity in other systems.

2.7.1 WATER CONTAINING SYSTEMS

The largest variety of known proton-conducting systems contain water. Although pure water consists of only two different elements, its structure and dynamics are very complex. The predominant intermolecular interaction is hydrogen bonding with an average energy of only ∼200 meV/bond. This weak interaction is very sensitive to fluctuations in pure water and, additionally, to static perturbations in water-containing systems. The high density of protons and their potentials, cause interactions leading to solvent effects. These comprise a rather high number of species, and the collective excitations are observed for aqueous hydrogen bonded networks in the microwave range. Comparable proton transfer, molecular diffusion, and reorientation rates is another consequence of that coupling. The complex scenario leads to the abundant variety in the phenomenology of proton transport in aqueous systems. Whereas pure water and ice are rather poor proton conductors under usual conditions, aqueous solutions of strong acids and solid acidic hydrates show the highest proton conductivities reported so far [35,36].

In pure water and ice, there is a strict association of two protons with one sp^3-hybridized oxygen thus forming neutral water molecules. At any finite temperature, protons are transferred within hydrogen bonds, i.e., charged protonic defects with respect to the perfect state are intrinsically formed because of water self-dissociation. The self-dissociation increases with increasing temperature. Obviously, proton

disorder in water is suppressed by strong solvent effects, and the stability of the sp^3 hybrid favors an ordered distribution of protons [37].

Under increasing pressure, however, the hydrogen bonds are successively compressed, which leads to a reduction of solvent effects. Under high pressure and temperature, the charge-carrier concentration in pure water may resemble that of a concentrated aqueous solution of a strong acid, however, with an equal concentration of protons and hydroxyl ions.

Apart from this intrinsic self-dissociation of water and ice, dissolved acids donate protons to the water solvent. This is especially relevant for water at surfaces (e.g., in particle hydrates) or in the cavities of porous materials such as zeolites. Owing to specific interactions with protons, such interfaces may stabilize or destabilize protons depending on their acid/base properties [35].

Layered acidic phosphates and phosphonates of zirconium have been investigated in their hydrated and dry form. In contrast to hydrates, these compounds showed some residual conductivity even after dehydration. The modification of such compounds by the introduction of -SO$_3$H containing groups in between the hydrated layers has recently led to conductivities close to that of NAFION.

There are many proton-conducting hydrates. They all have in common that the conductivity is related to the presence of water and that the host acts as a Bronsted acid toward the water of hydration, which is generally loosely bound in the structure. This retains the water of hydration up to temperatures slightly higher than the boiling point of water.

2.7.2 OXO ACIDS AND THEIR SALTS (SULFATES, SELENATES, PHOSPHATES, ARSENATES)

Oxo acids such as phosphoric acid (H_3PO_4), sulfuric acid (H_2SO_4), or perchloric acid ($HClO_4$) dissociate in aqueous solution, generating hydrated protons and thus proton conductivity. However, in the absence of water, i.e., in the anhydrous state, such acids may show appreciable proton conductivity (e.g., H_3PO_4, H_3OClO_4) which is due to their self-dissociation and conduction mechanisms. Despite investigations of numerous acidic salts of oxo acids, for a long time the proton conductivities observed were small. Their intrinsic conductivities are small with high activation enthalpies and some increase at low temperature upon doping.

The systematic search for fast proton conductivity in this family of compounds led to the discovery of the high conductivities of acidic iodates. This was followed by the discovery of the very high proton conductivity of cesium hydrogen sulfate, which has the ability to form a phase characterized by a high degree of dynamic reorientation disorder of the sulfate tetrahedra. Since this discovery, similar phase transitions have only been found for acidic salts with large cations [38].

Whereas $MHXO_4$ (M = Rb, Cs) exhibits fast proton-conducting phases for X = S and Se, only for the selenates of the $M_3H(XO_4)_2$ family have such phases been identified above phase transitions around 450 K. In most cases, the high-temperature phase has tetragonal or rhombohedral symmetry, but for some compositions another transition into a slightly more conducting cubic phase at higher temperature and pressure is observed. All of these compounds have in common that the proton is coordinated to oxygen of the XO_4 tetrahedra. These act to solvate the proton just like

the water does in water-containing systems. When there are more basic groups
available in the structure, the proton may also be coordinated to other moieties.

2.7.3 HIGH TEMPERATURE PROTON CONDUCTORS (OXIDES, HYDROXIDES, APATITES)

The oxide, which was the first shown to be predominantly proton conducting,
was acceptor-doped thoria for low p_{O2} (high p_{H2}) and temperatures above 1200°C.
The systematic investigation of the ionic conductivity of compounds with the
perovskite structure revealed several materials with pure oxide ion, mixed oxide
ion/proton, and pure proton conductivity in hydrogen or water containing
atmospheres. The highest proton conductivities, however, are observed in cerates and
zirconates, which also include the work on single crystals of acceptor doped $BaCeO_3$,
$SrCeO_3$, and $SrZrO_3$ [36].

Norby et al. [37] systematically studied proton conductivity in rare-earth oxides,
including La_2O_3 and Y_2O_3 within the framework of a consistent description of their
defect chemistry. Low proton conductivities were observed in acceptor-doped
tantalates ($KTaO_3$) and niobates ($LiNbO_3$). Acceptor doped titanates ($MTiO_3$, M = Sr,
Ba) are also poor proton conductors owing to their low proton concentrations, even
though the diffusivity of protons in these compounds was found to be extremely high.

The protonic defect in oxides corresponds to a hydroxyl ion on an oxygen site.
It is, therefore, appropriate to also include hydroxides into this family of proton
conductors. Proton conductivities have been reported for hydroxides of Na, K, Cs,
Mg, and Y.

Finally, phosphates with the structure of apatite ($Ca_5(PO_4)_3OH$) retain structural hydroxyl ions up to very high temperature (>1000°C) where some compounds with the apatite structure show appreciable proton conductivity.

2.7.4 ORGANIC/INORGANIC SYSTEMS

Acids like sulfuric acid (H_2SO_4) or phosphoric acid (H_3PO_4) form compounds in narrow composition ranges with organic molecules exhibiting basic groups. For instance, H_2SO_4 with triethylenediamine ($C_6H_{12}N_2$) and hexamethylenetetramine ($C_6H_{12}N_4$) leads to compounds with moderate proton conductivity [39]. Other studies focus on blends of oxo-acids with a variety of polymers. A blend of polyacrylamide and sulfuric acid has been found to display the highest conductivity within this family of compounds. This is, however, still lower than that of the pure acid. Blends of polyethylene oxide with ammonium salts have been shown to be proton conductors.

2.8 ADVANCES IN PROTON CONDUCTING GLASSES

Uma, Izuhara, and Nogami [40] developed P_2O_5-TiO_2-SiO_2 glasses using the sol-gel process and studied the effect of pore size on conductivity. The P_2O_5 concentration influenced their structures and thermal stability. The gels were studied using FTIR, nitrogen adsorption-desorption, TG/DTA and conductivity measurements. The proton conductivity of the P_2O_5-TiO_2-SiO_2 glass increased with increasing temperature in relative humidity of 90% and showed a maximum value of 3.6×10^{-2} S/cm.

Nogami, Goto, and Kasuga [41] investigated the effect of zirconium ion on glass structure, and proton conductivity for sol-gel derived P_2O_5-SiO_2 glasses. Porous glasses were prepared through hydrolysis of $PO(OCH_3)_3$, $Zr(OC_4H_9)_4$, and $Si(OC_2H_5)_4$. It was observed that the phosphorus ions, occurring as $PO(OH)_3$ in the Zr-free glass, became polymerized with one or two bridging ions per PO_4 unit with increased ZrO_2 content. The chemical stability of these glasses increased significantly with the addition of ZrO_2, but the conductivity gradually decreased from 26 to 12 mS/cm at room temperature.

Nogami et al. [42] prepared porous P_2O_5-SiO_2 glasses through a sol-gel route with varying percentages of P_2O_5 from 1 to 5% and SiO_2 from 100 to 95%, while the pore properties of the glasses were changed by controlling the preparation conditions. Proton conduction is associated with proton hopping between hydroxyl groups and water molecules. It was found that conductivity linearly increased with increasing the amount of surface area and the inverse of the pore radius. Protons in POH bonds displayed high conductivity, larger by ∼4 orders of magnitude than that in SiOH bonds. The highest conductivity was achieved for 5%P_2O_5-95%SiO_2 glass: 2×10^{-2} S/cm at room temperature.

Phosphosilicate glasses were prepared using both sol-gel and conventional melting methods, and proton conductivity of these glasses was investigated by Daiko [43]. Sol-gel derived glasses were found to be porous, and proton conductivity of these glasses increased by absorption of water. The dynamics of water molecules absorbed in nanopores are restricted, especially below 5 nm in pore radius, and proton mobility decreases with decreasing pore size. In contrast, at sub-zero temperatures, porous glasses with <1 nm pore radius, showed relatively high proton conductivities and at

such low-temperature proton conduction is not observed for polymer electrolytes. Glasses prepared by conventional melting showed very low proton conductivity because of their low carrier-density.

Nogami and Abe [44] studied the effect of molecular water on proton conduction and quantitatively analyzed the conductivity measurements of silica glasses with and without water molecules. The activation energy for conduction linearly decreased with increasing logarithm of proton concentration for glasses containing only protons as charge carriers and as the logarithm of the product of proton and water concentration for glasses containing both proton and water. Electrical conduction in glasses containing both protons and water molecules was associated with proton hopping between hydroxyl and water molecules, and its activation energy is related to the energy necessary for the dissociation of the proton from OH and H_2O.

2.9 EFFECT OF PHENYLTRIETHOXYSILANE IN SILICATE SYSTEMS

Bommel, Bernards, and Boonstra [45] investigated the influence of methyl-triethoxysilane (MTES) and phenyltriethoxysilane (PhTES) on the hydrolysis and condensation process of tetraethylorthosilicate (TEOS). The influence of the addition of differing amounts of MTES and PhTES was studied by viscosity measurements. When one of the four ethoxy groups in TEOS is replaced by a phenyl group the result is PhTES, which means that there are three groups that can hydrolyze and one group that is hydrolytically stable.

The fast hydrolysis-condensation processes of the alkyl-substituted ethoxy silanes contrast with the longer gelation time for the alkyl-substituted ethoxy silane-TEOS mixtures. However, due to the lower functionality of these compounds, there was less possibility of cross-linking during condensation. The greater influence of PhTES compared with MTES on lengthening the gelation time of TEOS mixtures is ascribed to the larger steric hindrance caused by the phenyl group [46]. It was found that the gelation process of such mixtures is slower than that of TEOS by itself. This is despite the fact that the hydrolysis rates and the condensation rates of PhTES and MTES by themselves are higher.

Rao, Kalesh, and Pajonk [46] reported experimental results on the hydrophobic and physical properties of TEOS based silica aerogels by incorporating PhTES as a synthesis component. The molar ratios of TEOS, ethanol, and water were kept constant while the molar ratio of PhTES/TEOS (M) was varied from 0 to 0.7. The hydrophobicity of the aerogels was tested by measuring the percentage of water uptake by the aerogels when exposed to 95% humidity at 40°C for 24 h and by measuring the contact angle, which varied from 120 to 130°. It was found that as the M value increased from 0.1 to 0.5, the hydrophobicity of the aerogels increased but the optical transmission decreased in the visible range. The thermal conductivity and the specific heat of the aerogels decreased with the increase in M values. In order to determine the thermal stability in terms of retention of hydrophobicity of the aerogels, they were heat treated in air in the temperature range of 25-600°C. The hydrophobic aerogels were found to be thermally stable up to a temperature of 520°C.

Jermouni, Smaihi, and Hovnanian [47] studied the hydrolysis and initial polycondensation of phenyltrimethoxysilane (PhTMS) and diphenyldimethoxysilane

(DPhDMS). Their study showed that DPhDMS, with its two reactive Si-O methyl bonds, enables the formation of linear chains, whereas the three hydrolyzable bonds of PhTMS can build a three-dimensional network. NMR was used to monitor the reaction mechanisms which occur during hydrolysis and condensation. Contrary to the observed behavior of tri- and tetra-functional alkoxides, the substitution of a methoxy group by a hydroxyl group induces a high-field shift whatever the hydrolysis ratio. The DPhDMS hydrolysis is much faster than that of PhTMS. This behavior is attributed to the electron-donating effect provided by phenyl side-groups. On the other hand, the condensation reactions are inhibited by the presence of the phenyl substituent and their kinetics decrease with the number of substituents.

Wu et al. [48] modified the surface of silica spheres with aminopropyl and phenyl groups. The particles modified with aminopropyl groups show the highest isoelectric point and the highest weight loss at 780°C because of the basic nature of aminopropyl groups and the higher reactivity of aminopropyl-triethoxysilane (APTES). The particles modified with the phenyl groups (PhTES) show the lowest water vapor adsorption because their surface is more hydrophobic than that of TEOS and APTES particles.

Jitianu and Klein [49] prepared melting gels with varying amounts of aliphatic (dimethyldiethoxysilane) and aromatic substitutions (PhTES). It was concluded that the phenyl groups are more polarizable, so increases in PhTES brings the polymer chains together, allowing for cross-linking and a decrease in the consolidation temperature. However, increases in PhTES increase the glass transition temperature as the phenyl groups disrupt the symmetry of siloxane chains.

III. EXPERIMENTAL TECHNIQUE

3.1 METHOD OF ATTACK

Alkoxides were used to prepare borosilicate xerogels of three different compositions: 85 wt.% SiO_2 – 15 wt.% B_2O_3, 80 wt.% SiO_2 – 15 wt.% B_2O_3. 75 wt.% SiO_2 – 15 wt.% B_2O_3 along with 5% and 10% phenyl modifications in the latter two compositions. Tetraethylorthosilicate (TEOS) was used as the source of silicon and boron was provided from two different sources – triethyl borate (TEB) and boric acid; separately for each composition and phenyltriethoxysilane (PhTES) was used to provide phenyl. The extent of time for hydrolysis reaction of TEOS to determine the appropriate time for the addition of boron precursor was derived from a previous study [4]. Once an alcogel was formed, various drying procedures were used to desiccate the alcogels into homogeneous xerogels. The characterization techniques listed below were used to monitor and study different properties of xerogels.

Thermogravimetric Analysis (TGA) was performed to monitor mass changes due to thermal events due to change in temperature.

Differential Scanning Calorimetry (DSC) was utilized to measure the temperatures and heat flows – exothermic and endothermic processes associated with the transitions in xerogels as a function of time and temperature in a controlled atmosphere.

X-Ray Diffraction (XRD) was used for qualitative analysis and to identify crystalline phases in the xerogels.

The electrochemical stabilities of the xerogels were studied by moisture adsorption/desorption cycles. The xerogels were subjected to humid atmosphere for brief time periods to monitor the mass gain due to adsorption with respect to time. The moisture adsorption was followed by placing the adsorbed xerogels into desiccators to study the mass loss with respect to time.

Electrochemical Impedance Spectroscopy (EIS) was performed at room temperature over a wide range of frequency to study the proton mobility in the xerogels.

3.2 GEL SYNTHESIS

The first step in the preparation of the borosilicate gels was the hydrolysis of TEOS ($Si(OC_2H_5)_4$). The TEOS was initially hydrolyzed because it has considerably slower hydrolysis rate than the boron alkoxide. The hydrolysis of the TEOS was accelerated by using a nitric acid catalyst. Ethanol was used as a mutual solvent for water and TEOS as they are immiscible.

TEOS and ethanol were mixed in equal volumes before any water was added for hydrolysis. As the TEOS and ethanol were continuously mixed on a stir plate, deionized water was added drop by drop to the previously hydrolyzed TEOS, and the molar ratio of alkoxide to water was maintained at 1:10 followed by addition of acid solution (0.1N HNO_3) of water. This reaction was carried out at room temperature for 1 hour.

Phenyltriethoxysilane (PhTES) was dissolved in ethanol, and this solution was added to the hydrolyzed TEOS solution for the compositions involving modification of the silicon precursor by phenyl groups followed by stirring for 10 minutes.

The amount of boron precursor used for the synthesis of borosilicate gels was kept constant for all compositions. Triethyl borate (TEB) was dissolved in ethanol, and this solution was added drop by drop to the previously hydrolyzed TEOS. Due to the moisture sensitivity of TEB, all glassware used in this procedure were rinsed with anhydrous ethanol.

After the addition of TEB, the mixture was stirred for 2 hours. This was followed by the addition of the remaining water needed to assist in removing the remaining alkoxy groups. The molar ratio of the alkoxides to water was always kept at 1:10. The solution was left to stir for 2 more hours before leaving it to gel and dry.

For the compositions involving boric acid as the boron precursor, boric acid was dissolved in ethanol and water such that the molar ratio of both boric acid to water and boric acid to ethanol was 1:10. An acid solution of 0.1N HNO_3 was used to accelerate the reaction. This solution was added to the previously hydrolyzed TEOS, and the mixture was allowed to stir for 4 hours before leaving it to gel and dry.

3.3 GEL DRYING

Prepared solutions were cast into glass vials and petri dishes. A key step to forming the homogeneous gels was to decrease the drying rate of the solution and to limit the contact with atmospheric humidity. This was either done by lightly capping

the glass vials or covering the petri dishes with an aluminum foil cover before placing

them in the drier.

Once, the gel was formed, the cap on the vial was completely loosened, or

more holes were pierced into the aluminum foil to facilitate the drying. The

temperature of the drying oven was between 55-60°C. By following this procedure,

transparent homogeneous gels were produced. Solutions placed directly in air for

drying or dried in the oven without a cover yielded inhomogeneous gels.

3.4 THERMAL ANALYSIS

Thermogravimetric analysis and Differential Scanning Calorimetry were

performed in NETZSCH Simultaneous Thermal Analyzer 449 F5. The powdered

samples were prepared by grinding a bulk piece of gel in an alumina mortar and

pestle. Samples were heated from room temperature to 500°C at a heating rate of

10K/min, and alumina crucibles were used as pans for the analysis. A blank run was

carried out utilizing the same parameters every time before the analysis to calibrate

the empty pan with respect to the reference pan.

3.5 X-RAY DIFFRACTION

PANalytical XRD was utilized for phase identification. The powder samples

were prepared using mortar and pestle, and the regular measurements were recorded

using sample flat stage settings (Bragg-Brentano). Match phase analyzer was used to

perform Rietveld analysis and quantify the amount of crystal phase present in the

samples.

3.6 MOISTURE ADSORPTION-DESORPTION

Adsorption tests were carried out in an enclosed, transparent Plexiglas® structure. A hole of appropriate size was drilled into this enclosure to fit the tube which guided water vapors from the source to the unit. A flask with a rubber stopper filled with tap water was used as a vapor source, with a small opening to fit the tube and avoid vapor loss. The beaker was placed on a hot plate, and the heating rate was kept constant for all the samples. A digital hygrometer was placed inside the enclosure to monitor the relative humidity along with the temperature inside the chamber. The samples were placed inside the humid atmosphere on reaching a relative humidity of 99%. The mass changes which represent the mass gain due to water adsorption were recorded in intervals of 5 minutes until the samples reached maximum water adsorption and no longer showed changes in mass.

Once the samples reached a plateau in weight, they were subjected to desiccation in calcium sulfate (Drierite®). The mass change representing the mass loss due to desorption was recorded until the samples no longer showed changes in mass.

3.7 ELECTROCHEMICAL IMPEDANCE SPECTROSCOPY

HP 4194A Impedance/Gain-Phase Phase analyzer was used for impedance spectroscopy measurements. The bulk samples were fragile and developed cracks on applying the silver conductor paste on the surface. To avoid this problem, the bulk samples were pulverized, and equal masses of each sample was collected. The powdered samples were pressed between two stainless steel disks (conductive

surface) in a pelletizer using polyvinyl alcohol as a binder. This configuration

allowed measurements to be performed over the frequency range 100Hz-10MHz.

IV. RESULTS

4.1 DRYING SOLUTIONS INTO XEROGELS

In Figure IV.1, a flow chart is shown outlining the different procedures used to turn solutions into alcogels and then to dry alcogels into xerogels. The chart delineates techniques that yielded either homogeneous or inhomogeneous xerogels. According to Figure IV.1, solutions placed in the laboratory atmosphere to dry produced a precipitate, forming an inhomogeneous gel. The precipitate was analyzed and found to be boric acid. When the gel was placed in a desiccator or into a dryer without capping or covering the container, the precipitate formed. It was observed that exposure to moisture and a faster drying rate contributed to the formation of boric acid precipitate.

The method used to desiccate a solution into a homogeneous xerogel involved lightly capping the container and placing the capped solution in a dryer until an alcogel was formed. After alcogel formation, the cap was loosened to facilitate the evaporation of water and alcohol vapors. By increasing the drying time from 24 hours to 72 hours (i.e., uncapped vs capped containers) and limiting the exposure to atmospheric moisture homogeneous xerogels were obtained. Alternatively, the solution was placed in a desiccator and allowed to form an alcogel. After the alcogel formation, it was removed from the desiccator, capped and then placed in a drier to complete the removal of alcohol and water and form a homogeneous xerogel. Of the two successful approaches used to form a homogeneous xerogel, the former was

utilized because of the excessive amount of time required for a solution to form an

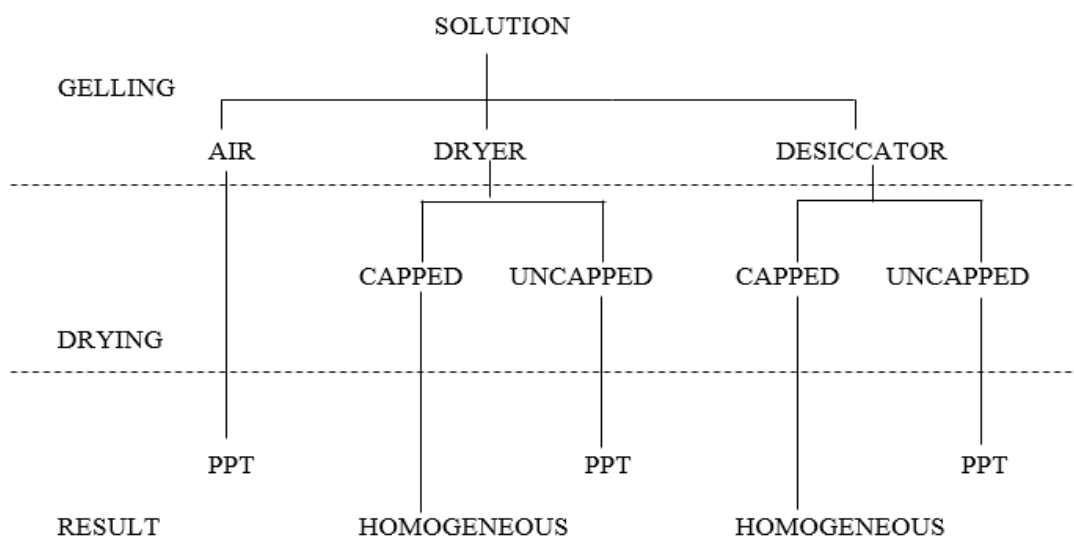alcogel when placed in a desiccator at room temperature.

Figure IV.1   Various procedures used to dry solutions into alcogels, and then alcogels into xerogels.

4.2 THERMAL ANALYSIS

Thermogravimetric analysis was performed in a nitrogen atmosphere to evaluate thermal stability and to measure the amount of volatile substances present in the gels. Samples were heated in an alumina crucible from room temperature to 500°C at 10K/min. Figure IV.2 shows the weight loss as a function of temperature for the gels prepared with TEB, and Figure IV.3 show the weight loss for the gels prepared with boric acid.

Table IV.1 shows the weight losses for all of the compositions. For the gels synthesized with TEB, the weight loss decreases from 18.35% to 13.36% as the PhTES substitution is increased from 0 to 10%. Gels prepared using boric acid show higher weight losses than those with TEB. For gels with boric acid, an increase in PhTES from 0 to 10% decreases the weight loss from 27.51% to 22.93%. In summary, the increase in the phenyl modifications to the silicon precursor decreases the total weight loss for both boron precursors.

Differential scanning calorimetry was performed simultaneously to monitor heat flow as a function of temperature and to predict the chemical reactions occurring in the gels as temperature was increase. Figure IV.4 show the DSC curves for gels prepared with TEB, and Figure IV.5 show the DSC curves for the gels prepared with boric acid.

The enthalpy changes for the endotherm peaks have been calculated, and the temperature ranges and enthalpy are presented in Table IV.2. The gels prepared with TEB show only one endotherm peak, whereas two or more peaks are observed for gels prepared using boric acid.

The increase in PhTES decreases the enthalpy values for both TEB and boric acid gels except for the sample composition 80% TEOS-15% Boric acid-5% PhTES.
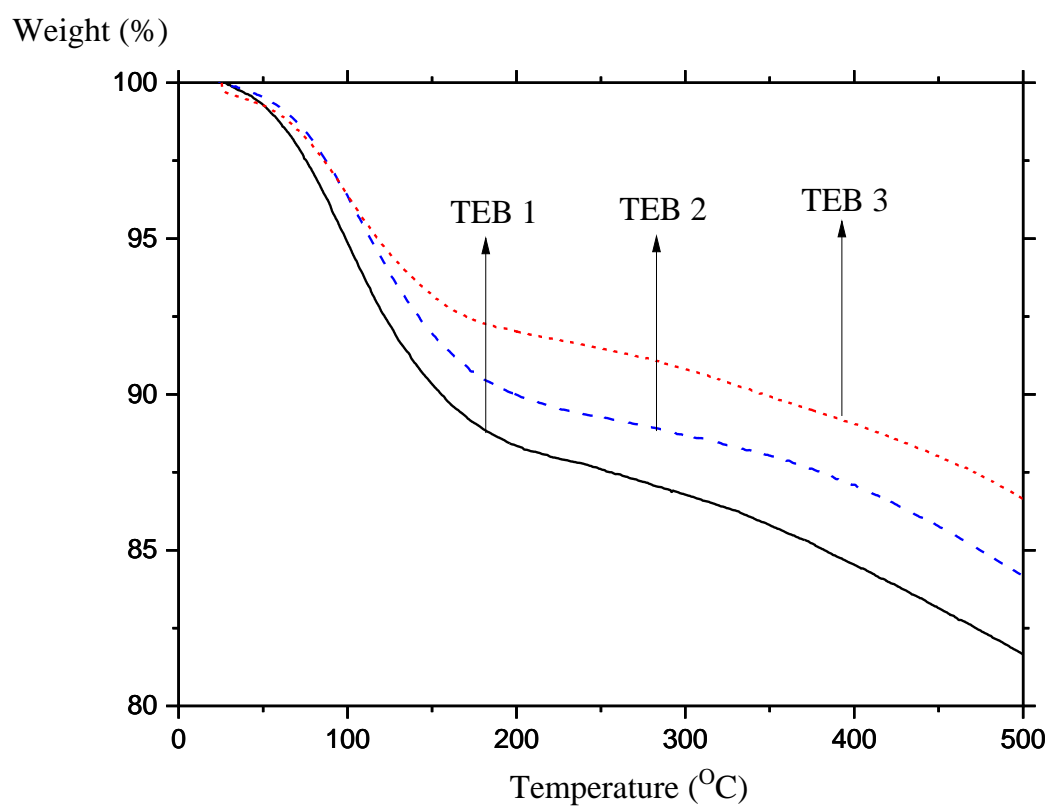
Weight (%)

Figure IV.2   Weight loss as a function of temperature for gels made from TEB.

TEB 1: 85% TEOS, 15% TEB

TEB 2: 80% TEOS, 15% TEB, 5% PhTES

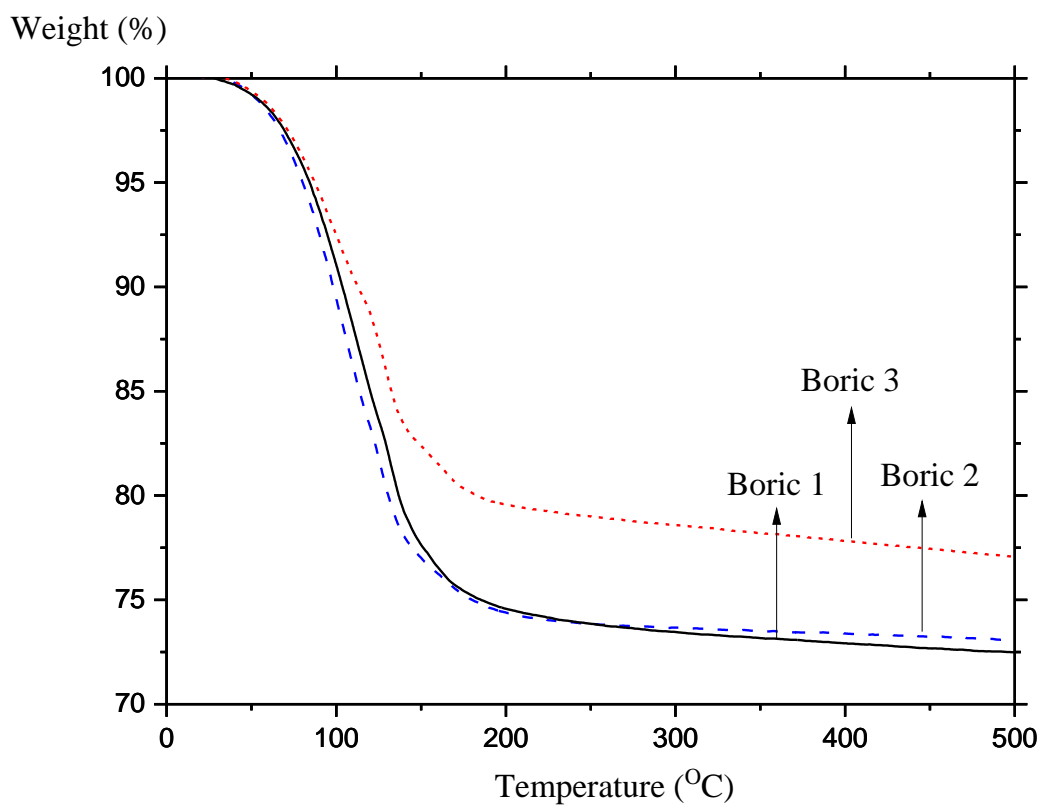TEB 3: 75% TEOS, 15% TEB, 10% PhTES

Figure IV.3   Weight loss as a function of temperature for gels made from boric acid.

Boric 1: 85% TEOS, 15% Boric acid

Boric 2: 80% TEOS, 15% Boric acid, 5% PhTES

Boric 3: 75% TEOS, 15% Boric acid, 10% PhTES

Table IV.1   Maximum Weight Loss for a given gel composition in the temperature range: 25-500°C.

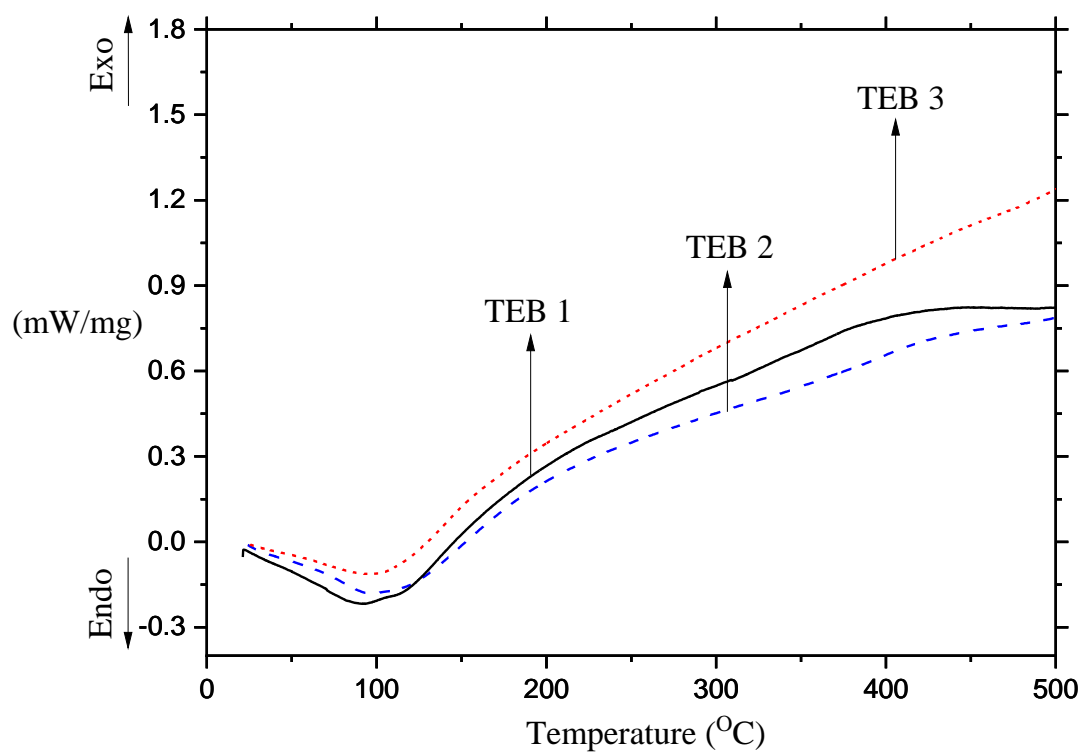| Composition	Weight Loss %
85%TEOS - 15%TEB	18.35
80%TEOS - 15%TEB - 5%PhTES	15.85
75%TEOS - 15%TEB - 10%PhTES	13.36
85%TEOS - 15%H_3BO_3	27.51
80%TEOS - 15%H_3BO_3 - 5%PhTES	26.91
75%TEOS - 15%H_3BO_3 - 10%PhTES	22.93

Figure IV.4   Heat flow as a function of temperature for gels made from TEB.

TEB 1: 85% TEOS, 15% TEB

TEB 2: 80% TEOS, 15% TEB, 5% PhTES

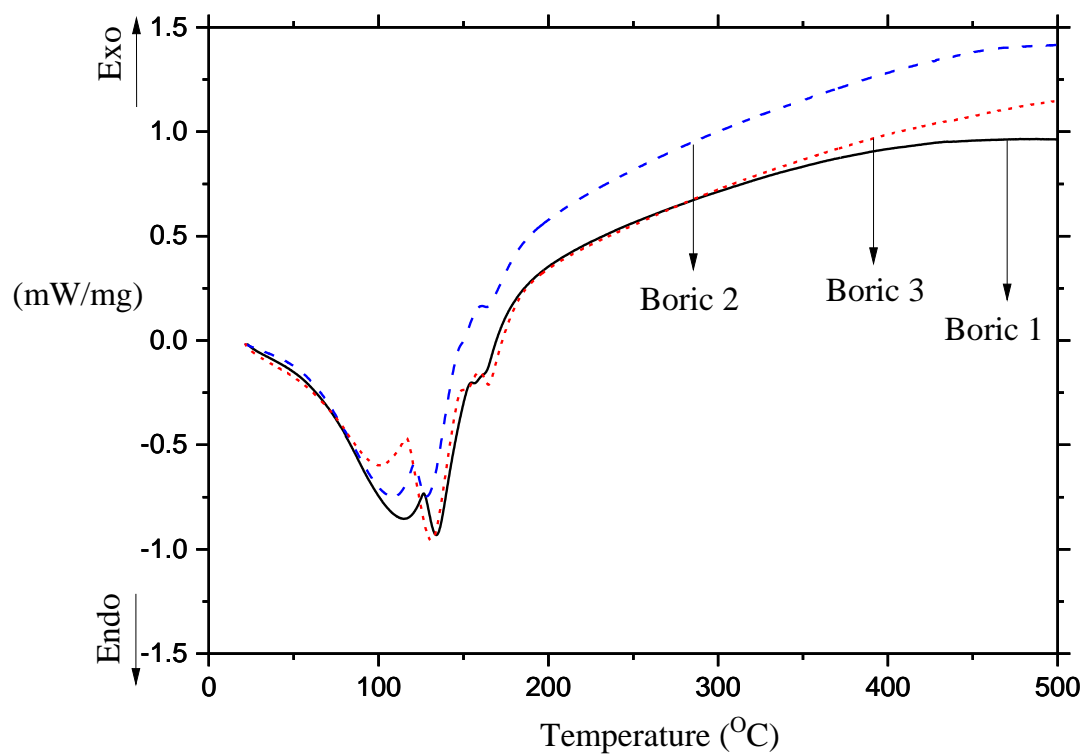TEB 3: 75% TEOS, 15% TEB, 10% PhTES

Figure IV.5   Heat flow as a function of temperature for gels made from boric acid.

Boric 1: 85% TEOS, 15% Boric acid

Boric 2: 80% TEOS, 15% Boric acid, 5% PhTES

Boric 3: 75% TEOS, 15% Boric acid, 10% PhTES

Table IV.2   Enthalpy changes for the given gel composition in the given temperature ranges.

Composition	Enthalpy Change (J/g)	Temperature Range (^{O}C)
85%TEOS - 15%TEB	-81.27	21 - 141
80%TEOS - 15%TEB - 5%PhTES	-78.62	24 - 150
75%TEOS - 15%TEB - 10%PhTES	-43.17	25 - 130
85%TEOS - 15% H_3BO_3	-383.11	22 - 170
80%TEOS -15% H_3BO_3 - 5%PhTES	-293.45	21 - 150
75%TEOS - 15%H_3BO_3 - 10%PhTES	-340.71	21 - 172

4.3 X-RAY DIFFRACTION

X-ray Diffraction analysis shows the precipitation of boric acid in the dried gels. Figure IV.6 shows the crystal phase in the gels prepared using TEB, and Figure IV.7 shows the crystal formation in the gels prepared using boric acid.

The increase in the PhTES decreases the amount of crystallinity for both boron precursors. Table IV.4 shows the intensity of the diffraction peak and the estimated amount of crystallinity. As the phenyl content is increased from 0 to 10%, the intensity (counts) of the diffraction peak decreases by about 30%.

The same trend is observed in the gels prepared using boric acid but with higher intensities, indicating higher amounts of crystallinity. As the PhTES is increased from 0 to 10%, the intensity of the diffraction peak decreased by about 50%.
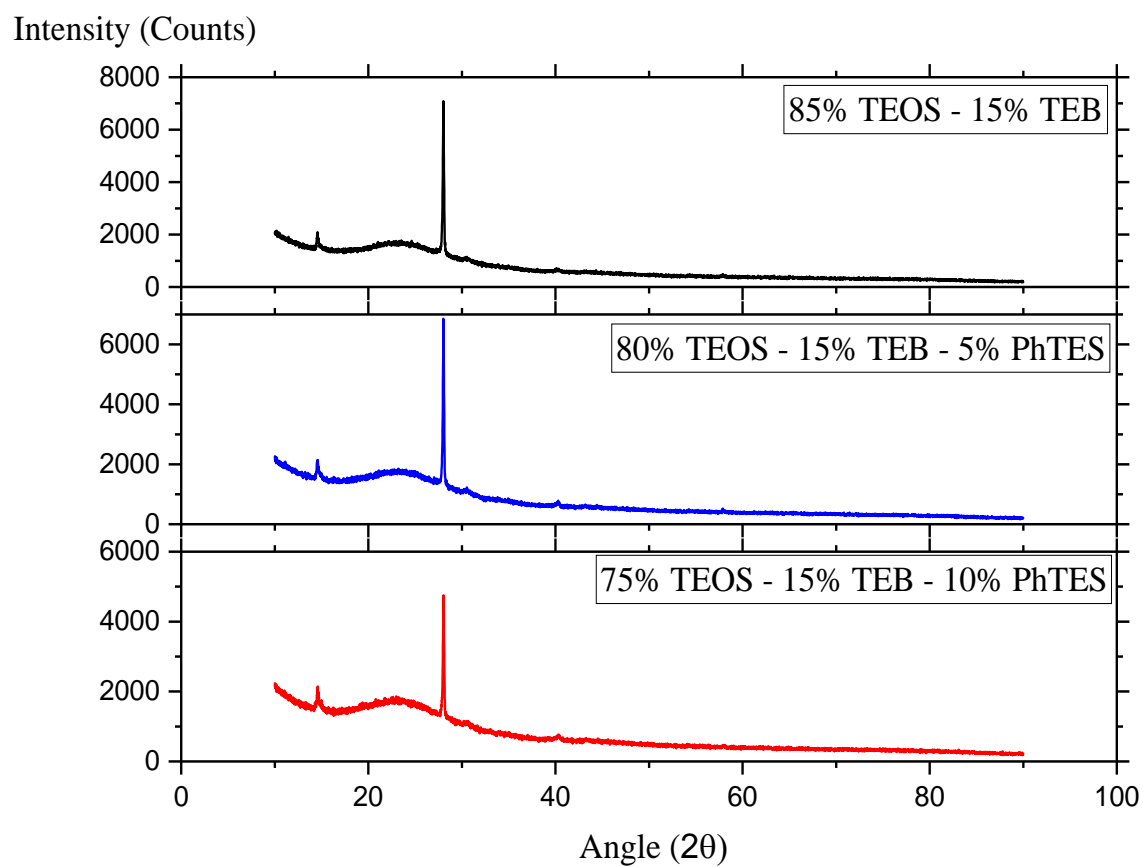
Figure IV.6   X-ray powder diffraction for gels made from TEB.
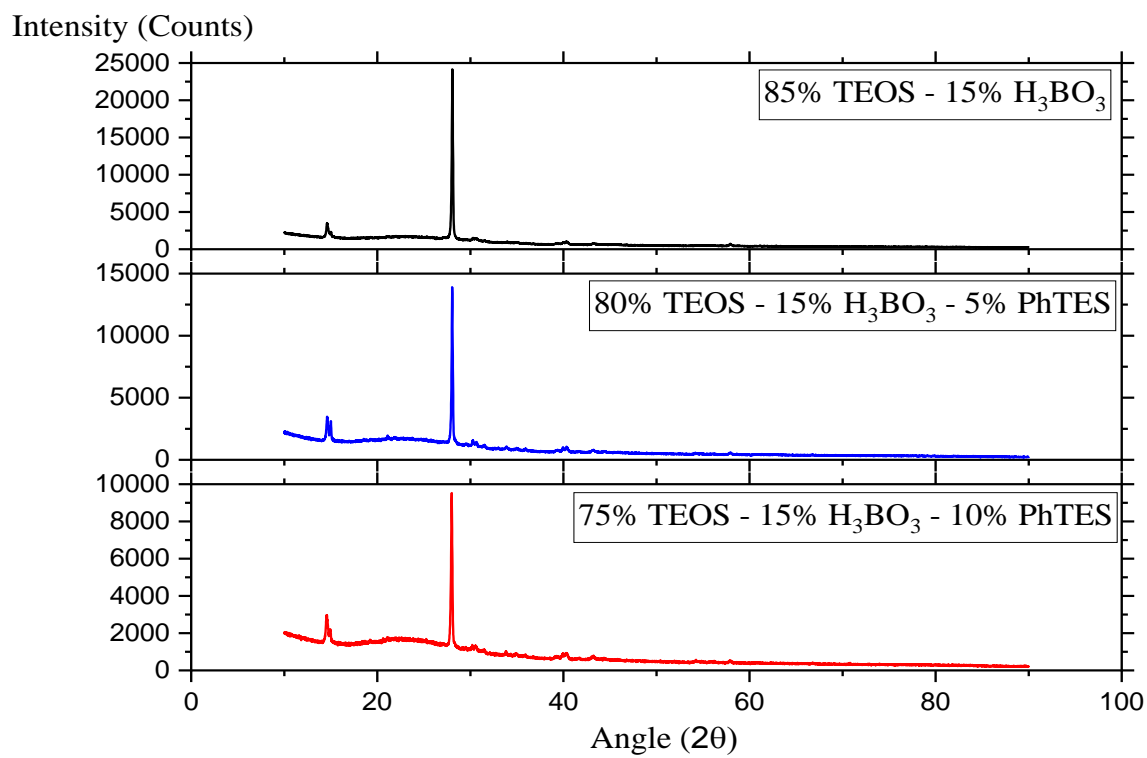
Intensity (Counts)

Figure IV.7   X-ray powder diffraction for gels made from boric acid.

Table IV.3   Maximum intensity of boric acid (counts) and the degree of crystallinity measured in the gels during X-Ray powder diffraction.

Composition	Boric Acid Intensity (Counts)	Degree of Crystallinity (%)
85%TEOS - 15%TEB	7084	4.75
80%TEOS - 15%TEB - 5%PhTES	6853	4.54
75%TEOS - 15%TEB - 10%PhTES	4749	3.84
85%TEOS - 15%H$_3$BO$_3$	24161	11.93
80%TEOS - 15% H$_3$BO$_3$ - 5%PhTES	13907	8.36
75%TEOS - 15% H$_3$BO$_3$ - 10%PhTES	9525	8.02

4.4 MOISTURE ADSORPTION-DESORPTION

The gels were placed in a sealed chamber as soon as the relative humidity reached 99%. Figure IV.8 shows moisture adsorption as a function of time by gels made with TEB. Figure IV.9 shows adsorption as a function of time by gels made with boric acid.

The changes in the mass were manually recorded at intervals of 5 minutes for the first hour, and then the changes were recorded at intervals of 10 minutes for the next hour. Gels synthesized without PhTES showed maximum adsorption for both boron precursors. As the PhTES content increased from 0 to 10%, the moisture adsorption gradually decreased from 8.0% to 5.37% for the gels prepared with TEB and 7.64% to 4.31% for the gels prepared with boric acid.

The gels reach their maximum moisture adsorption around 90-100 minutes when they are placed in an atmosphere of 99% relative humidity. After the gels reach maximum adsorption values, they were placed for desiccation in a container with calcium sulfate (Drierite®). There is an observable decrease in mass initially, but the rate of desorption slows down after 4 hours. Figure IV.10 shows the decrease in mass% as a function of time for the gels synthesized with TEB. Figure IV.11 shows the decrease in mass% as a function of time for gels prepared with boric acid.

As the PhTES content increases the amount of mass loss also increases for the gels synthesized with both boron precursors. The mass loss increases from -6.17% to -7.01% as PhTES increases from 0 to 10% for the TEB precursor gels, and for the gels prepared with boric acid, mass loss decreases from -5.25% to -7.62% as PhTES increases from 0 to 10%. Table IV.4 shows different parameters monitored during the experiments.

Figure IV.8   Percentage increase in the mass of the gels prepared from TEB as a function of time.

Figure IV.9   Percentage increase in the mass of the gels prepared from boric acid as a function of
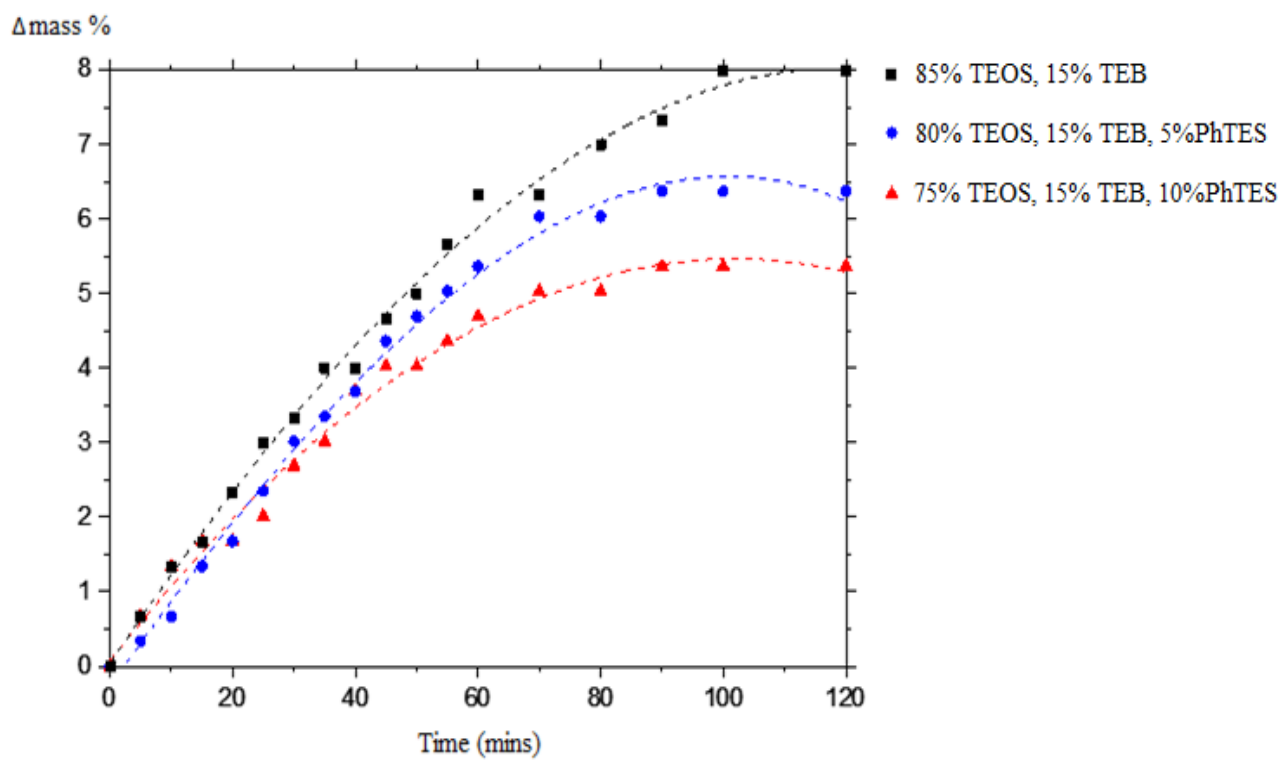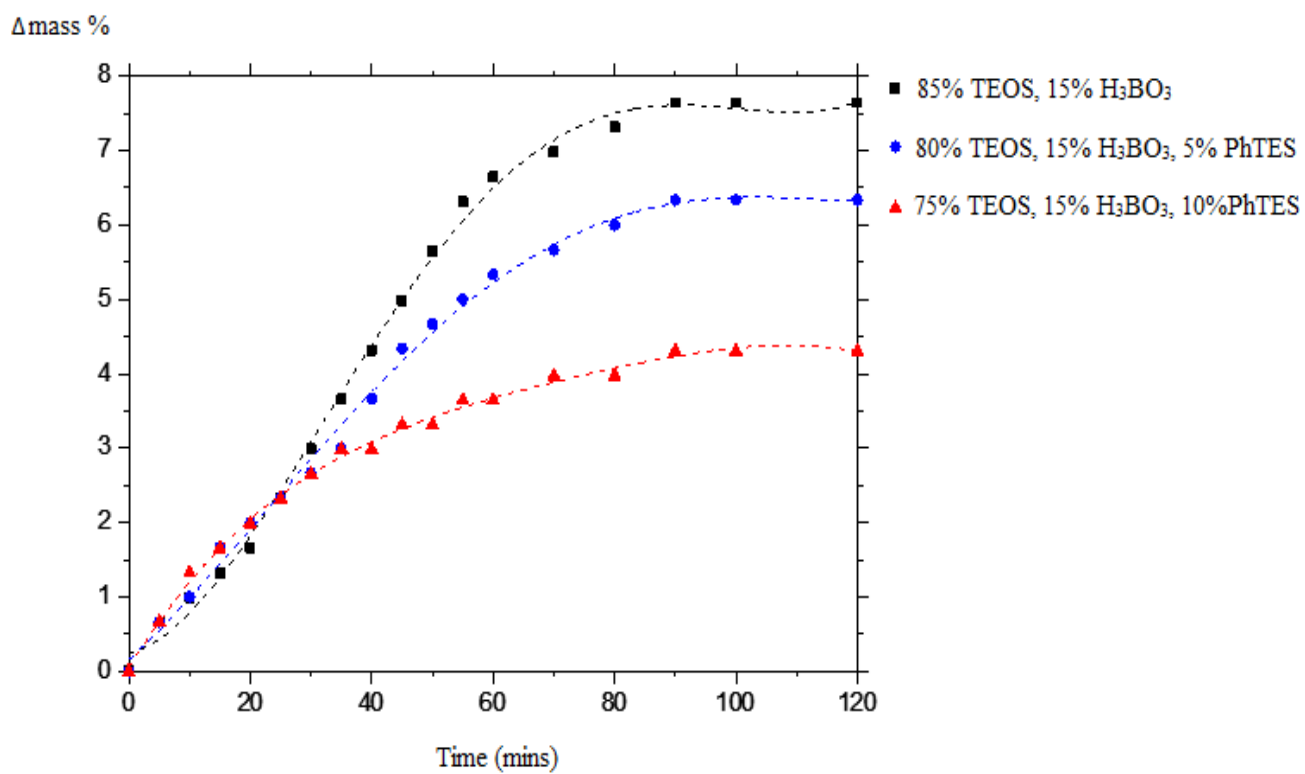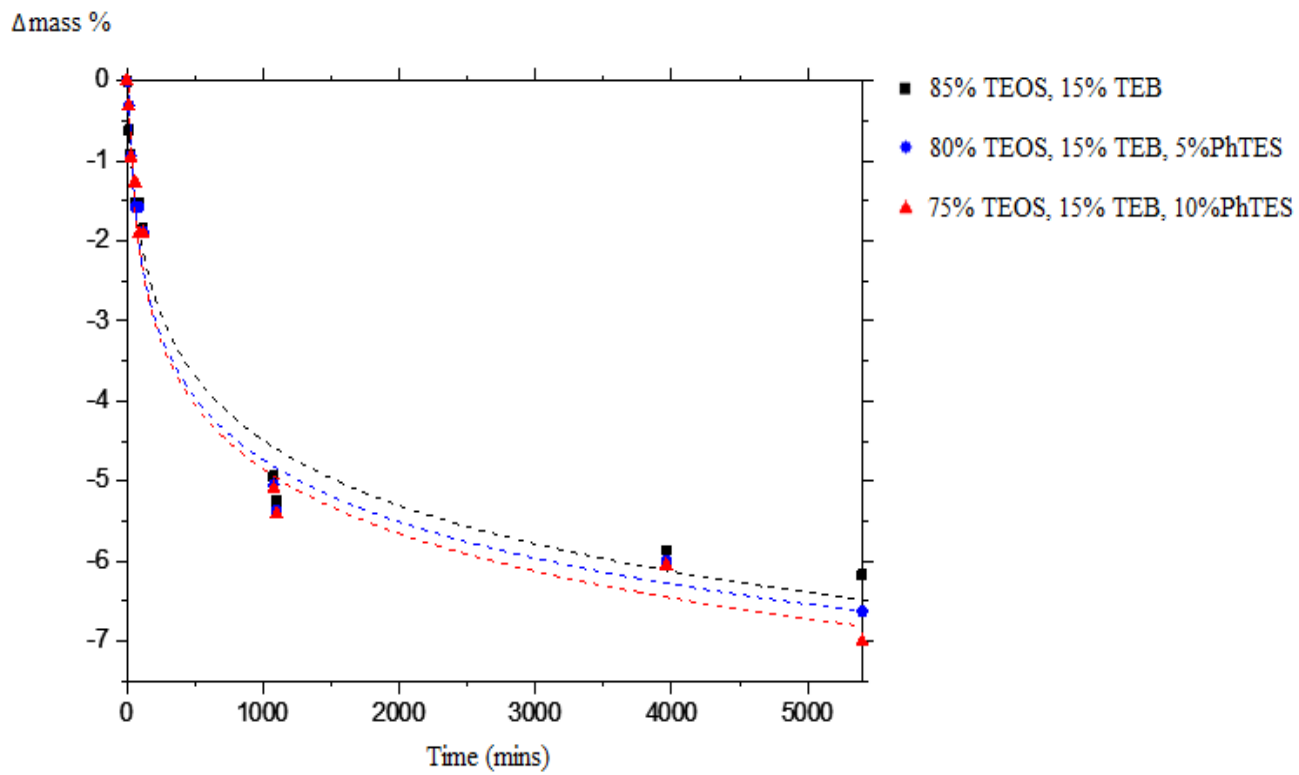
time.

Figure IV.10   Percentage decrease in the mass of the gels prepared from TEB as a function of time.
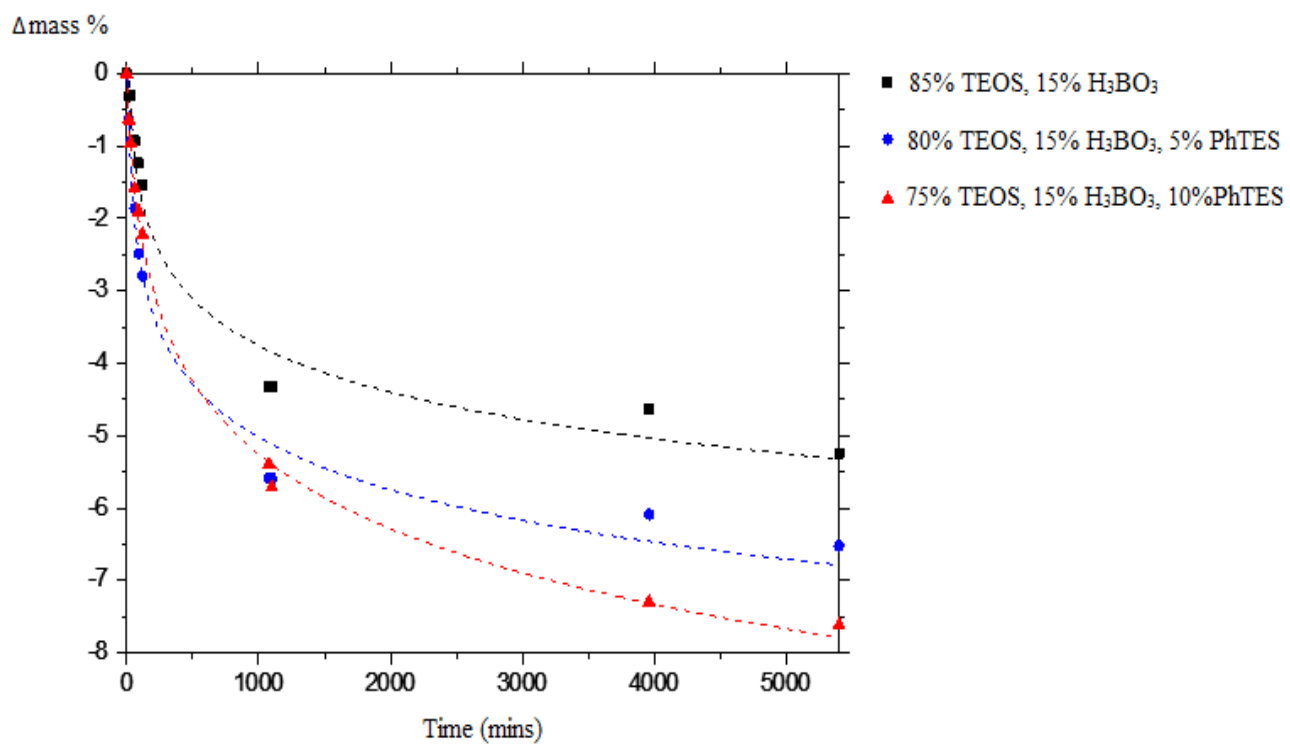
Figure IV.11   Percentage decrease in the mass of the gels prepared from boric acid as a function of time.

Table IV.4   Parameters monitored during the adsorption-desorption cycle.

Composition	Adsorption Saturation Time (mins)	Maximum Adsorption (% Mass Change)	Total Desorption (% Mass Change)	Difference: Adsorption-Desorption
85%TEOS - 15%TEB	100	8.00	-6.17	1.83
80%TEOS - 15%TEB - 5%PhTES	90	6.38	-6.63	-0.25
75%TEOS - 15%TEB - 10%PhTES	90	5.37	-7.01	-1.64
85%TEOS - 15%H_3BO_3	90	7.64	-5.25	2.39
80%TEOS - 15H_3BO_3 - 5%PhTES	90	6.33	-6.52	-0.19
75%TEOS - 15%H_3BO_3 - 10%PhTES	90	4.31	-7.62	-3.31

4.5 ELECTROCHEMICAL IMPEDANCE SPECTROSCOPY

The absolute impedance and the phase angles for the gels were recorded manually for all the gels. The quantities were measured over a frequency of 100 Hz to 10 MHz in intervals of 100 from 100 Hz to 1 KHz; intervals of 1 KHz between 1 KHz to 10 KHz; intervals of 10 KHz between 10 KHz to 100 KHz, intervals of 100 KHz between 100 KHz to 1 MHz and intervals of 1 MHz between 1 MHz to 10 MHz.

The real ($Z^{/}$) and imaginary ($Z^{//}$) parts of the impedance were obtained from the following equations:

$$Re(Z) = Z^{/} = |Z|*\cos\theta$$

$$Im(Z) = Z^{//} = |Z|*\sin\theta$$

Figure IV.12 shows the Nyquist plot ($Z^{/}$ vs. $Z^{//}$) for the gels prepared with TEB and Figure IV.13 shows the Nyquist plot for the gels prepared with boric acid. Figure IV.14 shows the Bode plot (Log (frequency) vs $Z^{/}$) for the gels synthesized with TEB and Figure IV.15 shows the Bode plot for the gels prepared with boric acid.

The ionic conductivity is calculated from the plots. It is assumed that the conductivity is all due to protons, because there are no other mobile species in these materials. Therefore, the conductivity is referred to as the proton conductivity.

The proton conductivity of the gels as a logarithmic function of frequency have been plotted in Figure IV.16 for the gels prepared with TEB and Figure IV.17 for the gels prepared with boric acid. In both cases, the proton conductivity decreases as the PhTES concentration was increased in the gels.

Table IV.5 shows the maximum proton conductivity recorded for the gels at room temperatures. The proton conductivity decreases from 1.83 mS/cm to 0.69 mS/cm as the PhTES content increases from 0 to 10% for gels using TEB, and for the boric acid, the conductivity decreases from 1.31 mS/cm to 0.61 mS/cm.
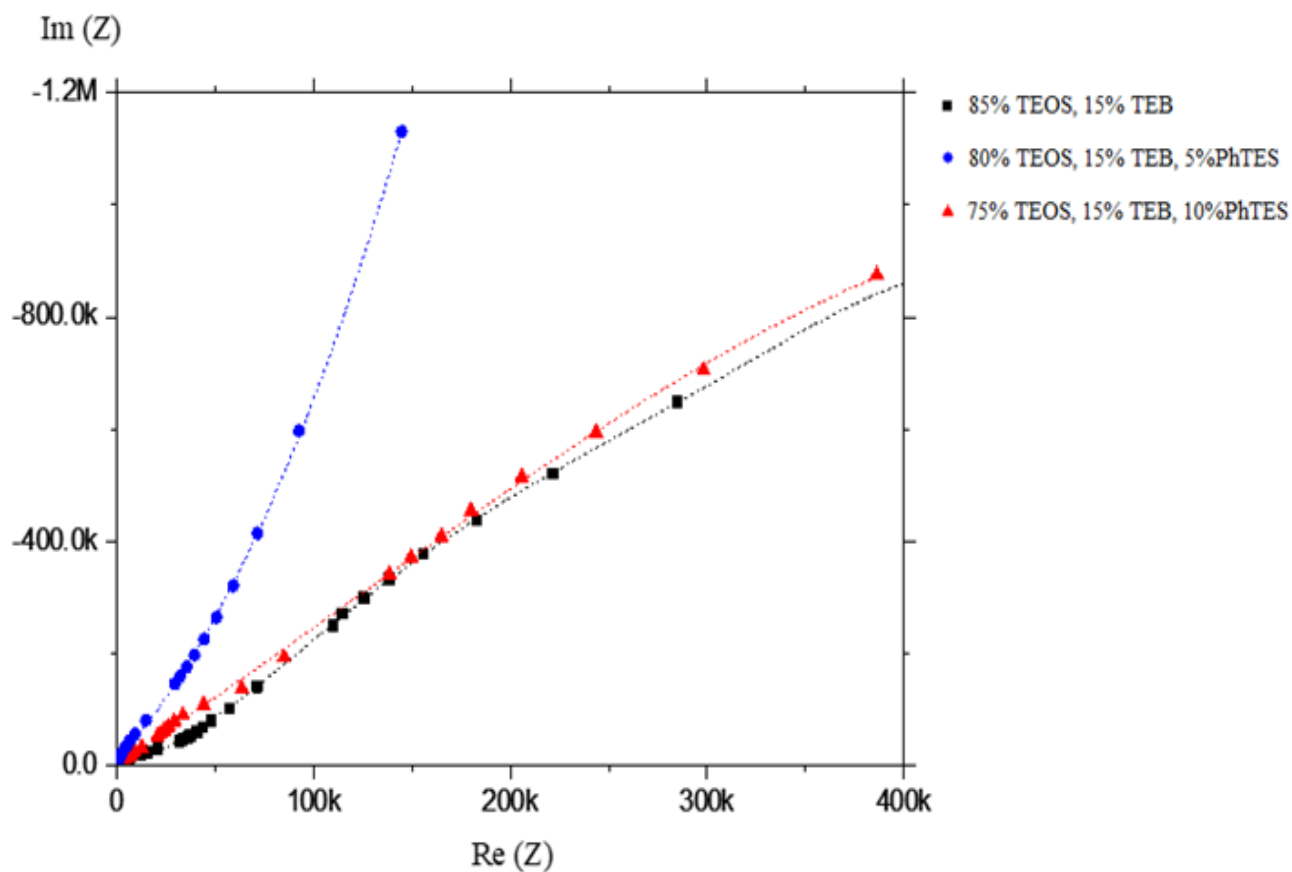
Figure IV.12   Nyquist plot showing the imaginary impedance plotted against the real impedance for

the gels synthesized from TEB.
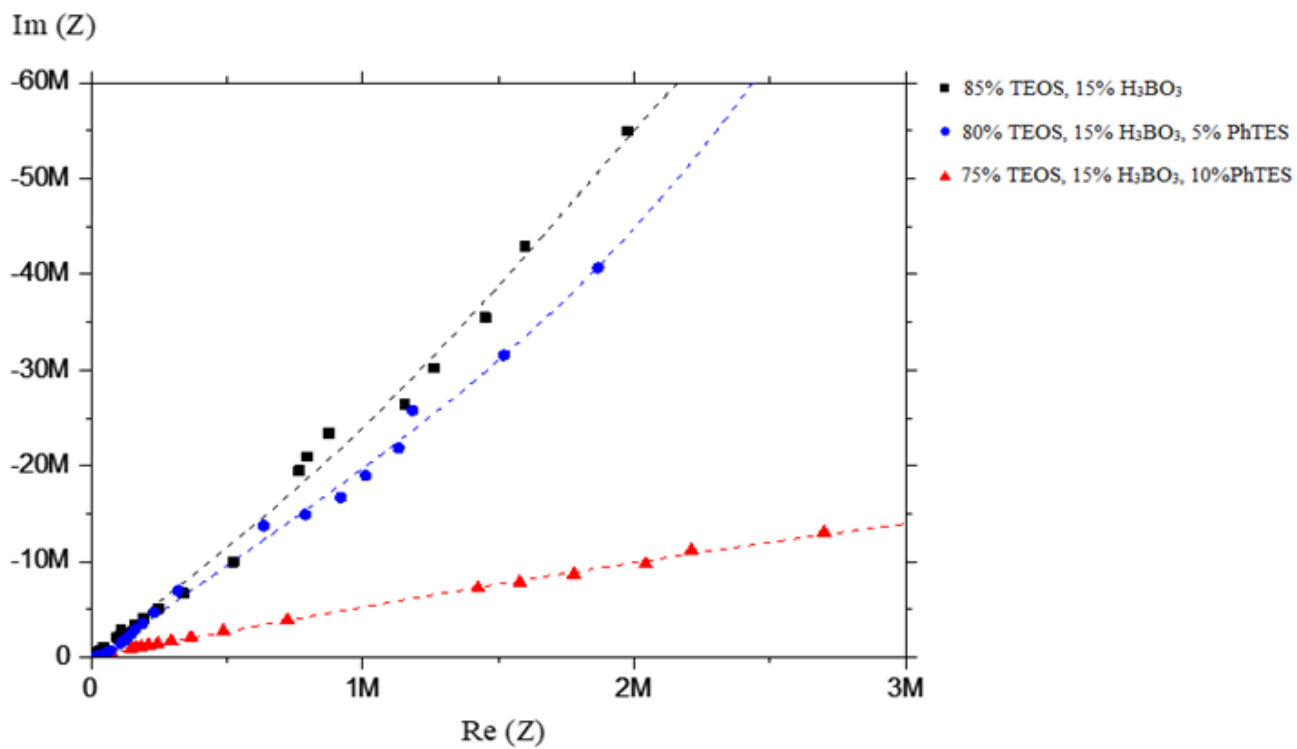
Figure IV.13   Nyquist plot showing the imaginary impedance plotted against the real impedance for the gels synthesized from boric acid.
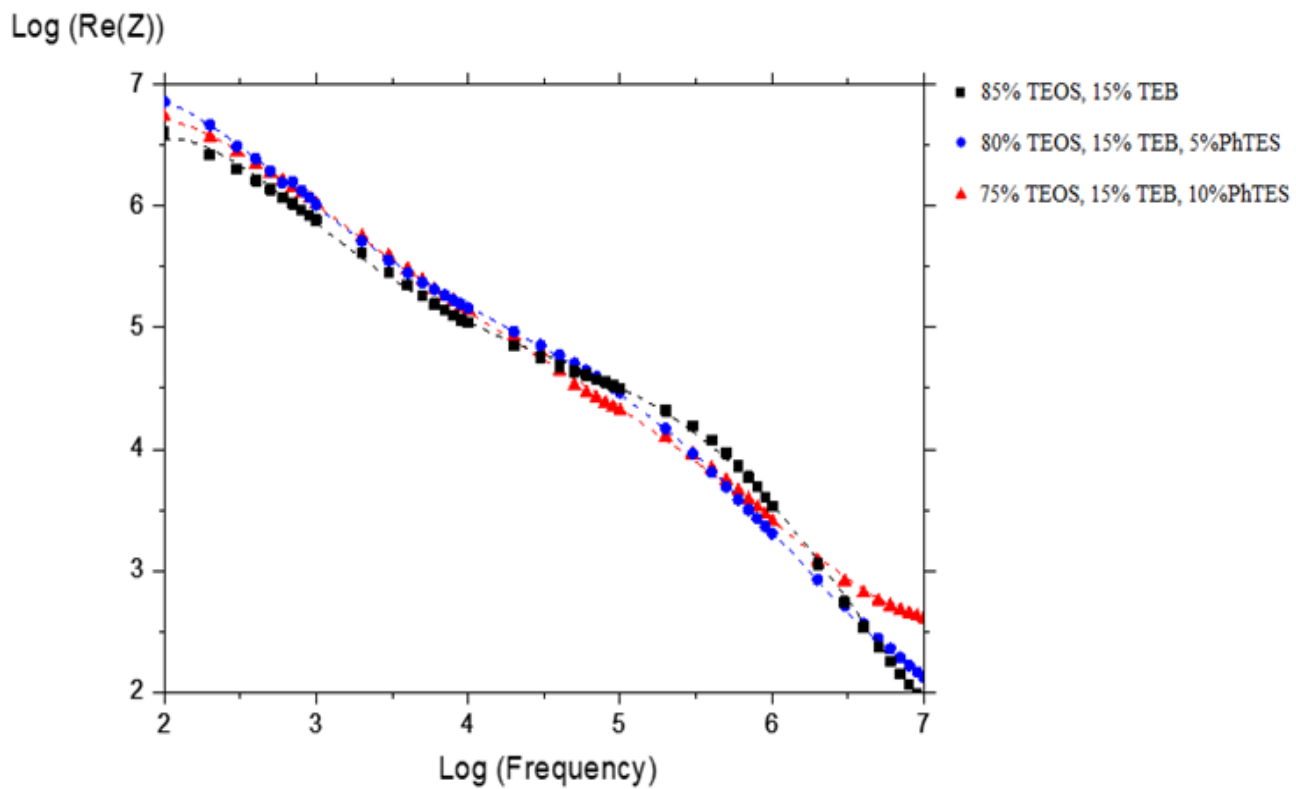
Figure IV.14   Bode plot showing the real part of impedance plotted against frequency on a

logarithmic scale for the gels synthesized from TEB.
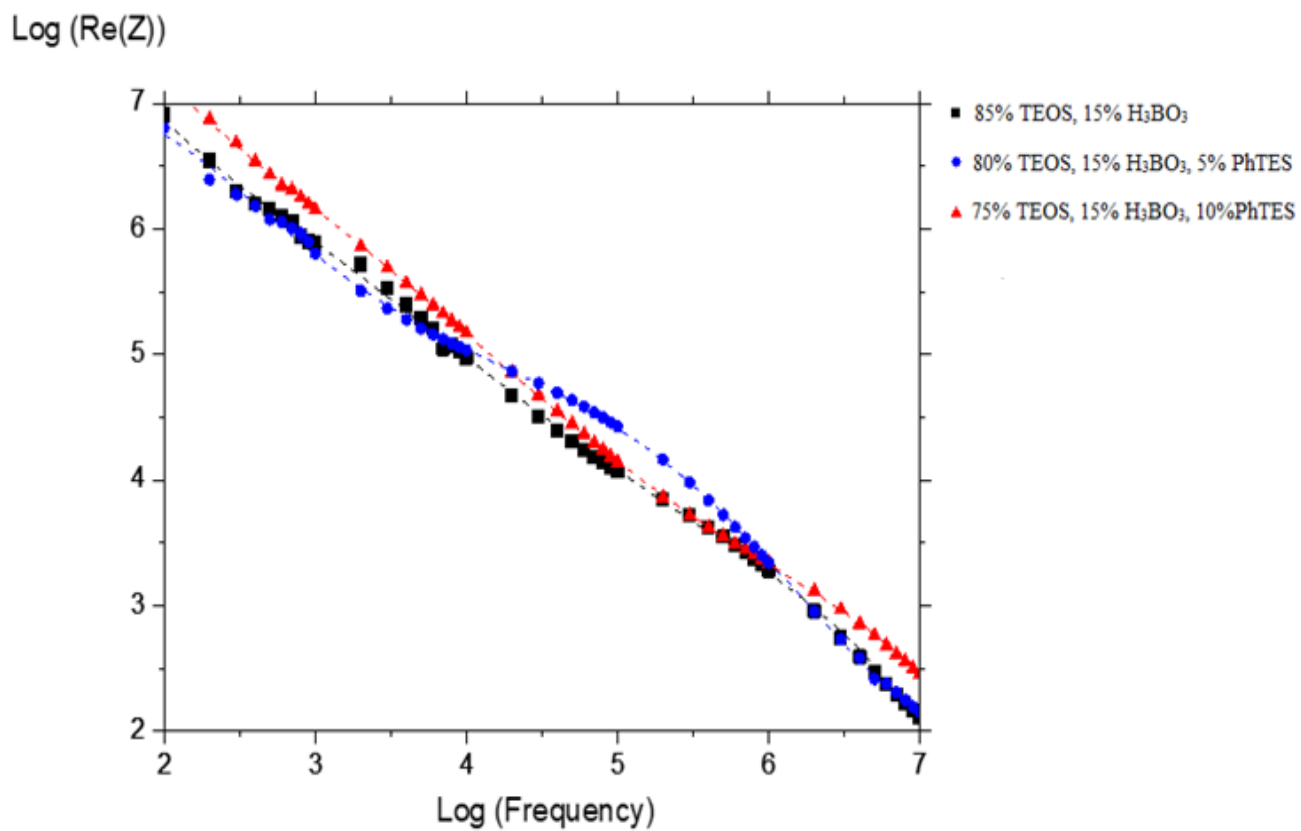
Figure IV.15   Bode plot showing the real part of impedance plotted against frequency on a logarithmic scale for the gels synthesized from boric acid.
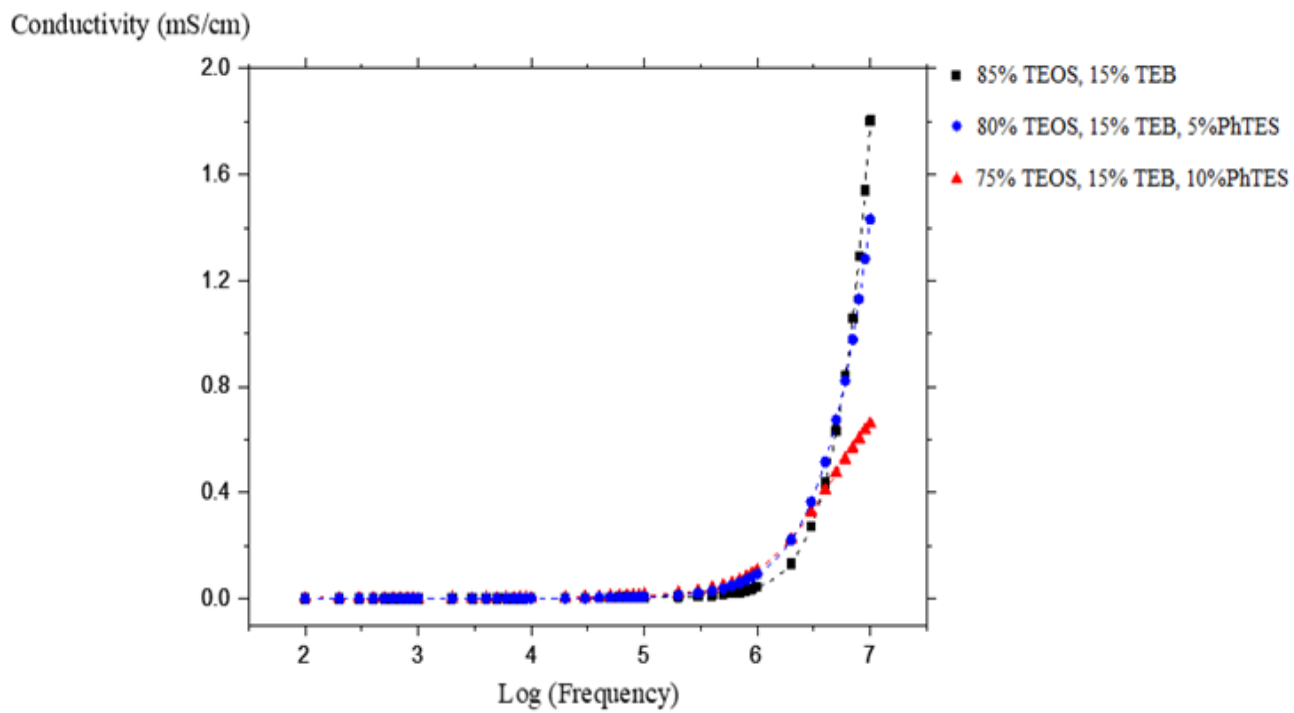
Figure IV.16   Proton Conductivity plotted as a logarithmic function of frequency for the gels synthesized from TEB.
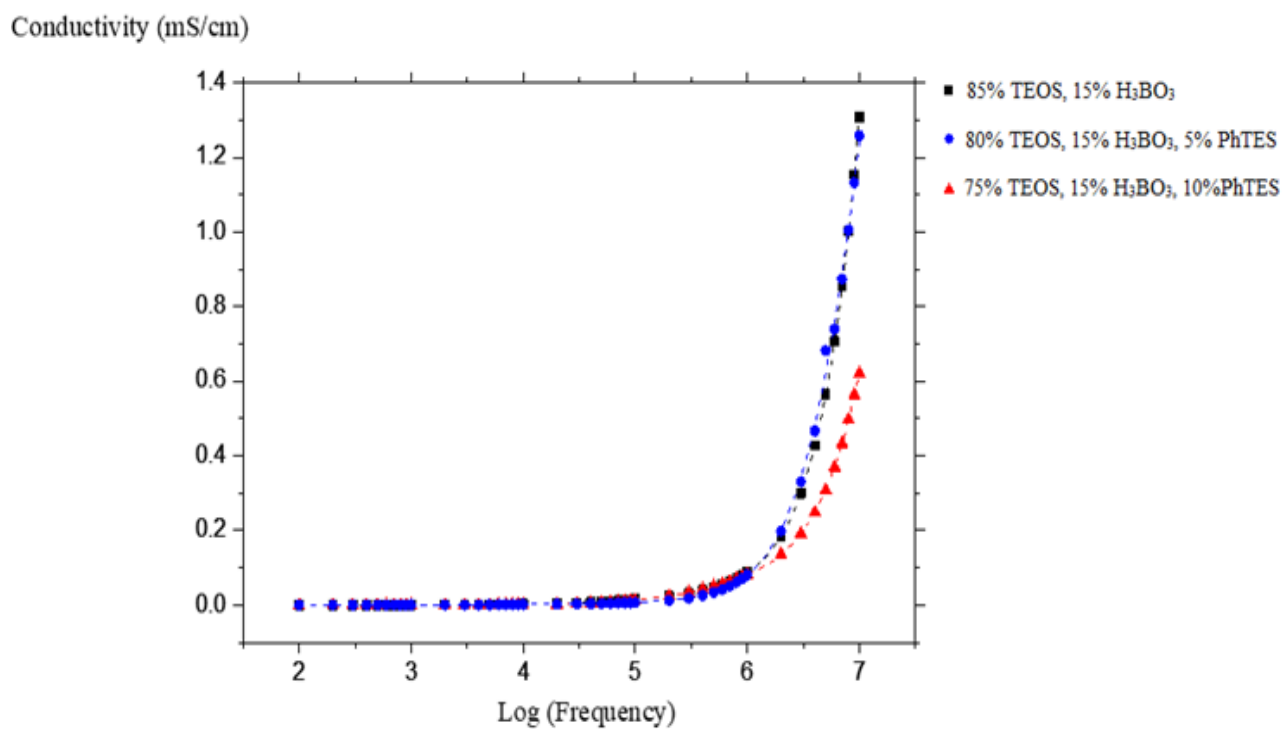
Figure IV.17   Proton Conductivity plotted as a logarithmic function of frequency for the gels synthesized from boric acid.

Table IV.5   Maximum proton conductivity recorded at room temperatures for a given
composition.

Composition	Maximum Proton Conduction (mS/cm)
85%TEOS - 15%TEB	1.83
80%TEOS - 15%TEB - 5%PhTES	1.42
75%TEOS - 15%TEB - 10%PhTES	0.69
85%TEOS - 15%H_3BO_3	1.31
80%TEOS - 15%H_3BO_3 - 5%PhTES	1.25
75%TEOS - 15%H_3BO_3 - 10%PhTES	0.61

V. DISCUSSION OF RESULTS

5.1 DRYING METHODS USED TO OBTAIN XEROGELS

A chart for various drying procedures used for drying the solutions into xerogels is shown in Figure IV.1. The chart shows some of the methods attempted to produce transparent xerogels while other routes yielded precipitation of boric acid on the surface.

When the alcogels were placed for drying in the laboratory atmosphere, the xerogels showed the formation of boric acid. For this procedure, the boric acid precipitate formed because of exposure to the atmospheric moisture.

Another technique that resulted in the formation of precipitate was to place the petri dishes and vials containing solutions directly into the dryer without capping them. In this instance, formation of precipitate was because of the faster drying rate. Even after the formation of the alcogel structure, there is still unreacted boron in the ethanol and water solution that surrounds alcogel. By drying too rapidly, the unreacted boron in the solution does not have enough time to react with the silanol groups. While ethanol and water are removed from the solution, the unreacted boron in the solution results in the formation of boric acid precipitate.

An approach that was successful in forming transparent xerogels involved lightly capping the solution container before placing them into the drier at 55 - 60°C. Once the alcogel was formed, the cap on the container was loosened to facilitate drying. By lightly capping the containers, the drying time increased to 72 hours,

compared to 24 hours for the uncapped solutions. By decreasing the drying rate, the

unreacted boron in the ethanol and water solution had enough time for reaction.

5.2 THERMAL ANALYSIS

The weight loss as a function of temperature for the gels prepared with TEB

can be seen in Figure IV.2 and those with boric acid in Figure IV.3. The addition of

phenyl groups reduces the total weight loss in both cases. Gels prepared using boric

acid show higher weight losses compared to comparable gels with same TEOS and

PhTES contents. Gels synthesized with TEB containing 0% PhTES show a weight

loss of 18.36%, whereas the same gel made with boric acid shows a higher weight

loss of 27.52%. Similarly, gels made with TEB, constituting 5% PhTES and 10%

PhTES show a weight loss of 15.86% and 13.36% respectively while the same gels

made with boric acid show higher weight losses of 26.92% and 22.93% respectively.

Table IV.1 shows the total weight loss (%) for the gels. The addition of

phenyl groups decreases the total weight loss in the gels. This trend can be attributed

to the decrease in volatile substances present in the gel. The drying stage is critical in

obtaining transparent and bulk gels. For this reason, all of the solution containers were

dried under the same conditions to be able to compare the effects of phenyl. An

increase of phenyl content appears to improve the solubility of the boron in the gel.

As a result, there is less unreacted boron present in the ethanol and water solution.

With the evaporation of ethanol and water during the drying stage, it appears that

there is less boric acid precipitation. In addition, TGA analysis shows lower residual

ethanol and water content in the gels with increasing PhTES content.

This fact can be further supported by the DSC results. Figure IV.4 shows the DSC curves for the samples synthesized with TEB. The magnitude of the first endotherm peak seems to decrease with the increase in phenyl content. Table IV.2 shows the enthalpy changes occurring in the mentioned temperature ranges. With an increase in phenyl content by 5%, the enthalpy change decreased from -81.27 J/g to -78.62 J/g and on further increasing the phenyl content by 10%, the enthalpy change, further dropped to -43.18 J/g. However, the same trend is not observed for the gels made with boric acid. As the PhTES content is increased from 0 to 5%, the enthalpy change decreases from   -383.12 J/g to -293.46 J/g. But further increasing the PhTES content from 5% to 10%, the enthalpy change increases from -293.46 J/g to -340.71 J/g. At first, this appeared to be an error, but on repeating the analysis, the same results were obtained.

The initial endotherm peak represents the heat absorbed by the gels to remove residual ethanol and water. The increase in the phenyl contents seem to decrease the enthalpy change except for gel composition 80% TEOS-15% boric acid-5% PhTES where the enthalpy change was larger compared to 75% TEOS-15% boric acid-10% PhTES. The decrease in the enthalpy change can be correlated with the decrease in weight loss obtained from TGA curves. The cause of the decrease in both the weight loss and the endotherm is associated with the decrease in volatile contents. It appears that increasing PhTES leads to improved solubility of boron and stronger interaction with the silanol groups. In turn, there is less boron loss in the solutions with substitutions of PhTES.

5.3 X-RAY DIFFRACTION

XRD patterns for the gels made with TEB can be seen in Figures IV.6 and with boric acid in Figures IV.7. All of the plots show crystal peaks at the same 2θ angle. Performing phase identification showed the displayed peaks were due to the boric acid precipitate.

Table IV.3 shows the intensity of the diffraction peak and the amount of boric acid present in the gels. The increase of phenyl groups reduces the amount of boric acid crystals in the gels. The amount of crystallinity almost doubles when boric acid is used to produce the same gels.

XRD analysis supports the thermal analysis, which showed lower boron loss with an increase in phenyl groups. There is less unreacted boron in the ethanol and water solution in gels with 5% and 10% PhTES. Consequently, less boric acid precipitates during the drying process.

5.4 MOISTURE ADSORPTION-DESORPTION

Figure IV.8 shows the adsorption as a function of time for the samples made with TEB and figure IV.9 shows adsorption as a function of time for samples made with boric acid. The total adsorption amounts are similar for both boron precursors. Figure IV.10 and Figure IV.11 show desorption of the TEB and boric acid gels respectively as a function of time. The mass losses due to desorption for the boric acid gels are comparatively higher for the same gels made with TEB.

Table IV.4 shows various parameters monitored during the adsorption/desorption cycle. During adsorption, when the gels reach maximum value,

they start to develop cracks. When the transparent and bulk gels were still left inside, they fractured with formation of boric acid precipitate on the surface. Gels synthesized with TEB containing 0% PhTES showed the highest adsorption value of 8% among all the samples. As the PhTES content was increased to 5% and 10%, the adsorption values for the gels were 6.38% and 5.37%. The same trend was observed for the gels made with boric acid. The adsorption value for 0% PhTES was 7.64%, for 5%PhTES the adsorption decreased to 6.33% and it was further decreased to 4.31% for the 10% PhTES gel.

The mass loss due to desorption increased with increasing phenyl content for all the gels. Gels made with TEB with no PhTES showed mass loss of -6.17% and with the increase in PhTES by 5% and 10%, mass loss increased by -6.63% and -7.01% respectively. The same pattern was observed for gels synthesized using boric acid. Mass loss increases from -5.25% to -6.52% to -7.62% as the phenyl content is increased from 0 to 5% to 10%. The difference between the mass gain due to adsorption and desorption indicates the samples without PhTES have the highest potential for retention of water.

5.5 ELECTROCHEMICAL IMPEDANCE SPECTROSCOPY

Figure IV.12 and Figure IV.13 show the Nyquist plots for the gels made with TEB and boric acid, respectively. Since, impedance is a complex function, increase in either the real or the imaginary part, increases the values of absolute impedance. Due to this reason and because of the nature of the samples, plotting the imaginary part of impedance against the real part did not generate a trend which could be correlated with the changes in the composition. For this reason, Bode plots were used

to monitor the changes in the real part of the impedance as a function of frequency on a logarithmic scale.

Figure IV.14 shows the Bode plots for the gels made with TEB and figure IV.15 shows Bode plots for the gels made with boric acid. Figure IV.14 shows that 5% PhTES gel made with TEB has the highest impedance at lower frequency. However, with increasing frequencies, gels containing 0% PhTES have the lowest impedance, followed by 5% PhTES and 10% PhTES gel. In contrast, the 5% PhTES gel has the lowest impedance at lower frequency, but at higher frequencies the same trend is observed as in the case of gels made with TEB.

The polarizing behavior in the impedance can be attributed to two reasons. Firstly, the nature of the sample preparation comes into consideration. Even after carefully weighing the samples and using equal amounts of polyvinyl alcohol, the method in which the gels react, and bind are very different, and this effects the impedance measurements, especially at lower frequencies. Secondly, at lower frequencies, there are considerable losses due to space charge polarization and due to the analyzing limitations of the analyzer.

Figure IV.16 and figure IV.17 show the proton conductivity of the gels made with TEB and boric acid, respectively plotted versus the frequency on a log scale. Table IV.5 shows the maximum proton conductivities measured at room temperature. It can be seen that with an increase in PhTES, the proton conductivity decreases for all of the gels. Among all of the gels, the maximum proton conductivity was recorded for the gel made with TEB with no PhTES. The conductivity decreased from 1.83 mS/cm to 1.42 mS/cm with increase in PhTES by 5%. The proton conductivity further decreases to 0.69 mS/cm on increasing PhTES by 10%. The proton

conductivity decreases for the gels made with boric acid with same compositions, but the decreasing trend persists. Gel containing 0% PhTES shows conductivity 1.31 mS/cm which reduces to 1.25 mS/cm and 0.61 mS/cm on increasing PhTES content by 5% and 10% respectively.

There are two explanations for these observations. Firstly, proton conductivity primarily occurs due to the hopping of H^+ ions. This hopping action increases with the increase of non-bridging oxygens in the matrix. There are many silanol groups in the gels. When the modified precursor is substituted for TEOS, there are fewer groups that can crosslink. However, the phenyl group is larger than a silanol, and it may have a steric effect that blocks the path of the proton. Secondly, proton conductivity occurs due to the transport of both H^+ and OH^- ions. As seen from the thermal and XRD analysis, increase in PhTES decreases the amount of residual ethanol and water present in the solution. As a result, the number of charge carriers decrease in the gel, and hence the conductivity decreases with increase in PhTES. While modifying the precursor limits the number of crosslinks, its effect is more complicated and needs further study.

VI. SUMMARY AND CONCLUSIONS

1.   Borosilicate xerogels were produced from metal alkoxides and acids with compositions: 85 wt. % TEOS - 15 wt. % TEB, 80 wt. % TEOS - 15 wt. % TEB - 5 wt. % PhTES, 75 wt. % TEOS - 15 wt. % TEB, 10 wt. % PhTES, 85 wt. % TEOS - 15 wt. % Boric Acid, 80 wt. % TEOS - 15 wt. % Boric Acid - 5 wt. % PhTES and 75 wt. % TEOS - 15 wt. % Boric Acid, 10 wt. % PhTES.

2.   The procedure used to dry alcogels into xerogels was a critical step in the formation of transparent and crack free gels. The atmosphere, as well as the rate of drying, were important. Exposure of the gels to atmospheric moisture during drying led to the formation of boric acid precipitate. Also, placing the alcogels into the dryer without capping the container yielded xerogels that contained a boric acid precipitate. By capping the alcogel before placing into a dryer and limiting exposure to atmospheric moisture yielded transparent bulk gels.

3.   Thermal analysis shows the increase of PhTES content increases the retention of boron in the silanol groups as the amount of material eliminated during heating decreased.

4.   XRD analysis shows the increase in PhTES is beneficial as it reduces the amount of crystallinity in the gels, and further affirming the improved retention of boron by the silanol groups.

5.   Moisture Adsorption-Desorption cycles show some hysteresis in the gels. While gels with no PhTES show highest water adsorption, they do not give up all of

the water during desorption. Also, adsorption in all gels reaches a maximum in 90 to 100 minutes. Desorption to a constant weight takes more than twice as long.

6.   Electrochemical Impedance Spectroscopy shows that the increase of PhTES decreases the proton conductivity slightly, due possibly to steric interference from the phenyl groups or a reduction of mobile protons.

7.   The gels synthesized with TEB are superior to the gels made with boric acid. The gels made with TEB show lower weight losses, lower amounts of crystallinity, higher moisture adsorption - lower mass loss during desorption, and higher proton conductivities.

REFERENCES

[1]   K-D. Kreuer, Proton Conductivity: Materials and Applications Chem. Mater. (1996) 8 610-641.

[2]   M. Nogami, Y. Daiko, T. Akai, and T. Kasuga "Dynamics of Proton Transfer in the Sol-Gel-Derived P2O5-SiO2 Glasses", The Journal of Physical Chemistry 105 (2001) 4653-4656.

[3]   Y. Daiko, T. Yamada, S. Yamanishi, A. Mineshige, and T. Yazawa, "Proton Incorporation, Mixed Alkaline Effect and H+/e− Mixed Conduction of Phosphosilicate Glasses and Glass-ceramics" Electrochemistry 82 (2014) 901-905.

[4]   J.W. Ryan, "Synthesis of Borosilicate Gels", PhD Thesis, Rutgers University - New Brunswick (1989).

[5]   C.J. Brinker and G.W Scherer, "Sol-Gel Science: The Physics and Chemistry of Sol-Gel Processing", Elsevier Science (2014).

[6]   S.P. Mukherjee, "Homogeneity of Gels and Gel-Derived Glasses", Journal of Non-Crystalline Solids 63 (1984) 35.

[7]   T. Hayashi and H. Saito, "Preparation of CaO-SiO$_2$ Glasses by the Gel Method", Journal of Materials Science 15 (1980) 1971.

[8]   S.P. Mukherjee, J. Zarzycki, and J.P. Traverse, "A Comparative Study of Gels and Oxide Mixtures as Starting Materials for the Nucleation and Crystallization of Silicate Glasses", Journal of Materials Science 11 (1976) 341.

[9]   R. Jabra, J. Phalippou, and J. Zarzycki, "Synthesis of Binary Glass-Forming Oxide Glasses by Hot-Pressing of Gels", Journal of Non-Crystalline Solids 42 (1980) 489.

[10]   E.M. Rabinovich, D.W. Johnson, J.B. MacChesney, and E.M. Vogel, "Preparation of High Silica Glasses from Colloidal Gels: I.", Journal of American Ceramic Society 66 (1983) 683.

[11]   H. Dislich, "New Routes to Multicomponent Oxide Glasses", Angewandte Chemie International Edition 10 (1971) 363.

[12]   I.M. Thomas, U.S. Patent No. 3 799 754 (1974).

[13]   B.E. Yoldas, "Monolithic Glass Formation by Chemical Polymerization", Journal of Materials Science 14 (1973) 1843.

[14]   D.C. Bradley, R.C. Mehrotra, and D.P. Gaur, "Metal Alkoxides", Academic Press (1978).

[15]   M. Russak, "Homogenization of Multicomponent Glasses", Journal of American Ceramic Society 61 (1978) 181.

[16]   M. Decottignies, J. Phalippou, and J. Zarzycki, "Synthesis of Glasses by Hot-Pressing of Gels", Journal of Materials Science 13 (1978) 2605.

[17]   S. Sakka and K. Kamiya, "The Sol-Gel Transition in the Hydrolysis of Metal Alkoxides in Relation to the Formation of Glass Fibers and Films", Journal of Non-Crystalline Solids 48 (1982) 31.

[18]   C.J. Brinker, K.D. Keefer, D.W. Schaeffer, R.A. Assink, B.D. Kay, and C.S. Ashley, "Sol-Gel Transition in Simple Silicates II.", Journal of Non-Crystalline Solids 63 (1984) 45.

[19]   B.E. Yoldas, "Modification of Polymer-Gel Structures", Journal of Non-Crystalline Solids 63 (1984) 145.

[20]   J. Zarzycki, M. Prassas, and J. Phalippou, "Synthesis of Glasses from Gels: The Problem of Monolithic Gels", Journal of Materials Science 17 (1982) 3371.

[21]   K. Matusita, T. Watanabe, K. Kamiya, and S. Sakka, "Viscosities of Single and Mixed Alkali Borate Glasses", Physics and Chemistry of Glasses 21 (1980) 78.

[22]   C.J. Brinker and G.W. Schere, "Relationships between the Sol-to-Gel and Gel-to-Glass Conversions", Ultrastructure Processing of Ceramics, Glasses, and Composites, Wiley Interscience 1984.

[23]   B.E. Yoldas, "Effect of Variations in Polymerized Oxides on Sintering and Crystalline Transformations", Journal of American Ceramic Society 65 (1982) 388.

[24]   B.E. Yoldas, "Introduction and Effect of Structural Variations in Inorganic Polymers and Glass Networks", Journal of Non-Crystalline Solids 51 (1982) 105.

[25]   R. J. Charles, "Mixed alkali effect in glasses" Journal of American Ceramic Society 48 (1965) 432-434.

[26]   J. M. Stevels, The electrical properties of glass, Encyclopedia of Physics (Springer) 4 (1957) 350-391.

[27]   W. E. Martinsen and T.D. McGee, "Effect of water content on electrical resistivity of Na2O-SiO2 glasses" Journal of American Ceramic Society 54 (1971) 175-176.

[28]   H. Scholze, and H. O. Mulfinger. "Der Einbau des Wassers in gläsern. V. die Diffusion des Wassers in Gläsern bei hohen Temperaturen." Glastech Ber 32 (1959): 381-385.

[29]   Y.H. Han, N. J. Kreidle and D. E. Day, "Alkali diffusion and electrical conductivity in sodium borate glasses: J. Non-crystal Solids 30 (1979)241-252.

[30]   K. Otto, "Electrical conducticvity of SiO2-B2O3 glasses containing lithium or sodium" Physics and Chemistry of Glasses 7 (1966) 29-33.

[31]   D. Ehrt and R. Keding, "Electrical Conductivity and Viscosity of Borosilicate Glasses and Melts", European Journal of Glass Science and Technology 50 (2009) 165-171.

[32]   J.J. Muray, "Surface Conductivity of Borosilicate Glass", Journal of Applied Physics 33 (1962) 1525-1531.

[33]   M.M.R.A. Lima, R.C.C. Monteiro, M.P.F Graca, and M.G. da Silva, "Structural, Electrical and Thermal Properties of Borosilicate Glass-Alumina Composites", Journal of Alloys and Compounds 538 (2012) 66-72.

[34]   H.H. Holzapfel, B. Wilfried, "Effect of Pressure and temperature on the Conductivity and Ionic Dissociation of Water up to 100 kilobars and 1000 degrees C", Journal of Chemical Physics 50 (1969) 4424-4428.

[35]   E. Tunkara, C. Albayrak, E. O. Polat, C. Kocabas, and O. Dag, "Highly Proton Conductive Phosphoric Acid-Nonionic Surfactant Lyotropic Liquid Crystalline Mesophases and Application in Graphene Optical Modulators" ACS Nano 8 (2014) 11007-11012.

[36]   S. Shin, H.H. Huang, M. Ishigame, and H. Iwahara, "Protonic conduction in the single-crystals of SrZrO3 and SrCeO3 doped with Y2O3" Solid State Ionics 40/41 (1990) 910-913.

[37]   T. Norby, O. Dyrlie, and P. Kofstad, "Protonic Conduction in Acceptor-Doped Cubic Rare-Earth Sesquioxides" Journal of American Ceramic Society 75 (1992) 1176-1181.

[38]   T. Takahashi, S. Tanase, O. Yamamoto, and S. Yamauchi, "Proton Conduction in Triethylenediamine and Hexamethylenetetramine Sulfate", Journal of Solid State Chemistry 17 (1976) 353-361.

[39]   T. Takahashi, S. Tanase, O. Yamamoto, and S. Yamauchi, "Proton Conduction in Triethylenediamine and Hexamethylenetetramine Sulfate", Journal of Solid State Chemistry 17 (1976) 353.

[40]   T. Uma, S. Izuhara, and M. Nogami, "Structural and Proton Conductivity Study of P_2O_5-TiO_2-SiO_2 Glasses", Journal of European Ceramic Society 26 (2006) 2365.

[41]   M. Nogami, Y. Goto, and T. Kasuga, "Proton Conductivity in Zr^{4+} Ion-Doped P_2O_5–SiO_2 Porous Glasses", Journal of American Ceramic Society 86 (2004) 1504.

[42]   M. Nogami, R. Nagao, C. Wong, T. Kasuga, and T. Hayakawa, "High Proton Conductivity in P2O5-SiO2 Glasses", Journal of Physical Chemistry 103 (1999) 9468.

[43]   Y. Daiko, "Proton conduction in glasses prepared via sol-gel and melting techniques", Journal of Ceramic Society of Japan 121 (2013) 539.

[44]   M. Nogami and Y. Abe, "Evidence of water-cooperative proton conduction in silica glasses", American Physical Society 55 (1997) 12108.

[45]   M.J. Bommel, T.N.M. Bernards, and A.H. Boonstra, "The Influence of the Addition of Alkyl-Substituted Ethoxysilane on the Hydrolysis-Condensation Process of TEOS", Journal of Non-Crystalline Solids 128 (1991) 231.

[46]   A. V. Rao, R. R. Kalesh, and M. Pajonk, "Hydrophobicity and Physical Properties of TEOS Based Silica Aerogels using Phenyltriethoxysilane as a Synthesis Component", Journal of Materials Science 38 (2003) 4407.

[47]   T. Jermouni, M. Smaihi, and N. Hovnanian, "Hydrolysis and Initial Polycondensation of Phenyltrimethoxysilane and Diphenyldimethoxysilane", Journal of Materials Chemistry 5 (1995) 1203.

[48]   Z. Wu, H. Xiang, T. Kim, M.S. Chun, and K. Lee, "Surface Properties of Submicrometer Silica Spheres Modified with Aminopropyltriethoxysilane and Phenyltriethoxysilane", Journal of Colloid and Interface Science 304 (2006) 119-24.

[49]   A. Jitianu, G. Gonzalez, and L.C. Klein, "Hybrid Sol-Gel Glasses with Glass-Transition Temperatures below Room Temperature", Journal of American Ceramic Society 98 (2015) 3673.